Abstract

SPECTROSCOPIC INVESTIGATIONS OF BINDING MECHANISMS BETWEEN ANTIMICROBIAL PEPTIDES AND MODELS OF THE MEMBRANES OF PSEUDOMONAS AERUGINOSA AND KLEBSIELLA PNEUMONIAE

by

Hanbo Chai

June 2014

Major Department: Chemistry

Department Chair: Dr. Allison S. Danell

Director of Thesis: Dr. Rickey P. Hicks

The wide application of antibiotics goes back over sixty years to the first use of penicillin in the mid-1940s. Antimicrobial agents have well-documented activity and have played a significant role in defending against various bacterial infections. However, antibiotic resistance has never ceased to undermine the efficacy of those compounds and has become a severe threat to patients with serious infections. It is imperative to discover and develop antibacterial agents with novel action mechanisms to lower the chance of drug resistance. A wide series of compounds called "antimicrobial peptides" (AMPs) have been either discovered in the nature or synthesized in laboratories around the world. The advent of AMPs has brought a new hope in the fight against the rise of antibiotic-resistant organisms.

Far-UV Circular Dichroism (CD) spectroscopy and ^{1}H NMR have been used to investigate the interactions of a series of synthetic, unnatural amino acid-containing AMPs with Lipopolysaccharide (LPS) isolated from drug resistant Gram-negative bacteria

Pseudomonas aeruginosa and *Klebsiella pneumoniae,* along with various phospholipid compositions to better approximate the chemical makeup of the membranes of these two strains. The results showed that: (1) the binding interactions between the AMPs and the membranes are defined by the physicochemical properties of the peptide and the membrane model; (2) binding of these AMPs to the lipid A region (the innermost and phospholipid-like layer) of the LPS is stronger and dominant compared with the binding with the O-polysaccharide outer leaf moiety; (3) when different compositions of phospholipids were incorporated into the LPS to make a complete membrane model of the two strains, wavelength shifts in the CD spectra of the AMPs were observed that represents conformational changes of AMPs upon binding with the membrane model.

SPECTROSCOPIC INVESTIGATIONS OF BINDING MECHANISMS BETWEEN ANTIMICROBIAL PEPTIDES AND MODELS OF THE MEMBRANES OF PSEUDOMONAS AERUGINOSA AND KLEBSIELLA PNEUMONIAE

A Thesis

Presented To

the Faculty of the Department of Chemistry

East Carolina University

In Partial Fulfillment

Of the Requirements for the Degree

Master of Science in Chemistry

by

Hanbo Chai

June , 2014

SPECTROSCOPIC INVESTIGATIONS OF BINDING MECHANISMS BETWEEN ANTIMICROBIAL PEPTIDES AND MODELS OF THE MEMBRANES OF PSEUDOMONAS AERUGINOSA AND KLEBSIELLA PNEUMONIAE

by

Hanbo Chai

APPROVED BY:

DIRECTOR OF THESIS: _____

(Rickey P. Hicks, PhD)

COMMITTEE MEMBER: _____

(William E. Allen, PhD)

COMMITTEE MEMBER: _____

(Colin S. Burns, PhD)

COMMITTEE MEMBER: _____

(Anthony Kennedy, PhD)

COMMITTEE MEMBER: _____

(John M. Kenney, PhD)

CHAIR OF THE DEPARTMENT OF CHEMISTRY:

_____

(Allison S. Danell, PhD)

DEAN OF THE GRADUATE SCHOOL:

_____

Paul J. Gemperline, PhD

TABLE OF CONTENTS

LIST OF TABLES

LIST OF FIGURES

LIST OF ABBREVIATIONS

Ala alanine……..9

AMP antimicrobial peptide……...6

Arg arginine……...58

Beta-Ala β- alanine……35

CD circular dichroism……7

Dab diaminobutionic acid……13

DPC dodecylphosphocholine……..10

Dpr diaminopropionic acid……13

ESKAPE *Enterococcus faecium*, *S. aureus*, *Klebsiella pneumoniae*, *Acinetobacter baumannii*, *Pseudomonas aeruginosa*, *Enterobacter*.....2

ESP electrostatic surface potential maps……...10

FDA The Food and Drug Administration……2

FMOC fluorenylmethyloxycarbonyl protecting group…….16

Fpa 4-fluorophenylalanine……..13

GABA 4-aminobutanoic acid……13

Gly glycine……13

HTS High Throughout Sequencing……...2

INH Isoniazid……2

KDO 3-deoxy-D-mannooctulosonic acid……..20

LPS lipopolysaccharides……...3

Lys lysine……...13

MDR multidrug-resistant……2

MDR-TB multidrug-resistant tuberculosis……...2

MIC minimum inhibitory concentration…….62

MRSA methicillin-resistant S. aureus……...3

NMR Nuclear Magnetic Resonance…….10

Nph 4-nitrophenylalanine……34

Oic octahydroindolecarboxylic acid…….13

Orn 2,5-diaminopentanoic acid……...13

Phe phenylalanine…….13

POPC 1-Palmitoyl-2-Oleoyl-sn-Glycero-3-Phosphocholine……16

POPE 1-Palmitoyl-2-Oleoyl-sn-Glycero-3-Phosphoethanolamine……..16

POPG 1-Palmitoyl-2-Oleoyl-sn-Glycero-3-[Phospho-rac-(1-glycerol)]……..16

RMP rifampicin…….2

SDS sodium dodecyl sulfate……...7

SUV small unilamellar vesicles……16

t-BOC tert-butyloxycarbonyl protecting group…….16

Tic tetrahydroisoquinolinecarboxylic acid……..13

UTIs urinary tract infections……...4

VISA vancomycin-intermediate *S. aureus*……5

VRSA vancomycin-resistant *S. aureus*……6

CHAPTER 1: BACKGROUND INFORMATION

1.1 Drug Resistant Bacteria：Evolution and Medical Issues

1.1.1 A Brief History of Drug Resistant Evolution

Drug resistance of bacteria is not a recent phenomenon, having accompanied almost the entire history of antibiotics discovery and development. Dating back to 1937, the sulfonamides were applied as the first generation of antimicrobial treatments and shortly thereafter drug resistance specific to sulfonamides was observed [1]. Before the introduction of sulfonamides, the most famous and widely used antibiotic, penicillin, was discovered by the future Nobel laureate Sir Alexander Fleming. Several years after 1940 this β-lactam compound had saved millions of people's lives who had war wounds and other infections in World War II [2]. However, this powerful antibiotic was not resistance-free even at the primitive stage of therapeutic application. Before penicillin was formally introduced as an antibacterial agent, an enzyme which can deactivate and degrade penicillin was discovered and identified in some bacteria species including *Balantidium coli* [3]. This observation suggested that resistance had naturally existed among the bacterial population before large scale antibiotic application made it so apparent.

Throughout the history of antibiotic discovery and development, there are several important time points [1]. Penicillinase was discovered at almost the same time with penicillin during early 1940s; the golden age began in the 1950s when a large number of antibiotics were found, identified and used. This group of drugs also primarily formed the modern arsenal still used today. The advent of molecular biology in the 1960s facilitated a molecular level understanding of the role of drug resistance genes found in bacterial genomes,

but drug-resistant genomes imbedded in bacterial genomes became to be selected and enhanced by various antibiotics at an increasing speed since then [1]. Important research methods, such as pharmacologic, biochemical, target enzyme specific and more recent genomic HTS (High Throughout Sequencing) have worked together to improve the use of antibiotics by modifying dosing, understanding drug resistance mechanisms, designing new compounds and predicting potential antibiotic action targets [1]. Another time point worth mentioning is the establishment of the FDA Office of New Drugs after the famous pharmaceutical scandal caused by the notorious teratogen thalidomide, making the new drug registration much stricter and slower. Meanwhile, during the years from the late 1960s to 2000, drug resistance increased significantly due to heavy use of those compounds. The rapid advancements of synthetic chemistry made the industrial large-scale production a less challenging process and remarkably lowered the price of those compounds. People manufactured them easily, and underuse, overuse, and misuse contributed significantly to the acceleration of gene mutations and the selection of resistant strains [1].

1.1.2 Drug Resistant Bacteria of Medical Significance

Infectious human diseases bacteria have turned into multidrug-resistant (MDR) forms as a result of inappropriate antibiotic use [1]. An important MDR pathogen is multidrug-resistant tuberculosis (MDR-TB), which is known for being resistant to isoniazid (INH) and rifampicin (RMP), two major first-line anti-TB drugs [4]. There are several medically significant bacterial strains of interest, including *Enterococcus faecium*, *S. aureus*, *Klebsiella pneumoniae*, *Acinetobacter baumannii*, *Pseudomonas aeruginosa*, *Enterobacter* species, know collectively as ESKAPE for abbreviation [5].

Among the ESKAPE, *Enterococcus faecium* and *S. aureus are* Gram-positive bacteria. Gram-positive bacteria are characteristized by a thick, porous cross-linked peptidoglycan layer on the top of cytoplasmic lipid layer [6]. *Enterococcus faecium* can be either innocuous, existing in human gastrointestinal tract, or be pathogenic, when found in surgical wound infection and urinary tract infection in hospitals [7]. When being multidrug-resistant, especially to vancomycin, it is referred to VRE [8]. *S. aureus* is a widely distributed bacterium that commonly infects human respiratory tract. This bacterium has notorious fame throughout infection treatment history, ranging from pimples to lethal pneumonia, toxic shock syndrome and sepsis. It is one of the major nonsocomial infections and American hospitals alone treat approximately 500,000 patients every year for staphylococcal infection [9]. *S. aureus* had developed high percentage of in-hospital resistance to penicillin after only fifteen years of wide application of the antibiotic [10]. The greatest threat brought by *S. aureus* is know as MRSA, or Methicillin-resistant *S. aureus,* which can be resistant to most β-lactam antibiotics. MRSA is now a problem in hospitals. Unfortunately there are only several families of antibiotics, such as glycopeptides antibiotic vancomycin, can treat MRSA with a relatively good outcome. However, even vancomycin is not the permanent standing line since recently MRSA isolates associated with decreased susceptibility to glycopeptides have been reported [11].

By comparison, the membrane structure of Gram-negative bacteria is more complex due to its lipopolysaccharide (LPS)-containing outer membrane. A peptidoglycan layer is still present but is much thinner than that of Gram-positive bacteria, lying between an LPS outer membrane and plasma membrane. LPS is an amphiphilic molecule that consists of three parts:

a highly variable hydrophile O-antigen, core oligosaccharide, and highly conserved hydrophobic lipid A [12]. The sugar sequence of O-antigen can vary from strain to strain [13]. The infections brought by Gram-negative bacteria can be severe because LPS is an endotoxin that can bind with cell types of the human immune system to induce a strong immune response, promoting the excessive release of cytokines and consequently causing septic shock [14]. Therefore it's more challenging to treat Gram-negative bacterial infections and extra attention should be paid to those with multidrug resistance.

On our bacterial interest list, *Klebsiella pneumoniae*, *Acinetobacter baumannii*, *Pseudomonas aeruginosa* and *Enterobacter* species are Gram-negative. It is no surprise all of the four have developed multidrug resistance and become major causes of many nosocomial infections [15]. *Acinetobacter baumannii* is well known in military units, and its multidrug resistance spread into civilian hospitals because of transportation of wounded soldiers [16]. *Enterobacter* is an opportunistic pathogen which infects hospitalized, immunocompromised patients with urinary tract infections (UTIs), intra-abdominal infections, endocarditis, etc. *Pseudomonas aeruginosa* and *Klebsiella pneumoniae* are focus of this thesis project. The former is typically opportunistic and nosocomial, naturally has a wide spectrum of antibiotic resistance, and causes a series of hospital-acquired infections including pneumonia, septic shock, urinary tract infection, and gastrointestinal tract infection. Patients with cystic fibrosis, skin burns, and premature infants are always highly endangered groups [17]. Lastly, *Klebsiella pneumoniae* causes deadly Klebsiella pneumonia, which gradually damages the human lungs through inflammation and hemorrhage. Severe cell death and so-called "currant jelly sputum" are the results. Immunocompromised patients are more susceptible to this

infection.

1.2 Potential Solution to Drug Resistance: Antimicrobial Peptides (AMP)

The wide application of antibiotics has been going on for over sixty years since the first use of penicillin. Those antimicrobial agents have well-documented activity and have played a significant role in defending against various bacterial infections. However, antibiotic resistance continues to undermine the efficacy of those compounds and has become a severe threat to patients with serious infections. As previously stated, the fast growth of antibiotic resistance during the later half of the 20^{th} century is a result of human selection by abusing and misusing traditional antibiotics [1].

The specificity of traditional antibiotics can be a double-edged sword; specificity allows one antibiotic to be active against one or a similar series of microorganisms using a unique mechanism of action. For instance, penicillin belongs to the family of β-lactam antibiotics, which inhibit peptidoglycan sythesis of bacteria cell wall. This target-specificity makes the antibacterial spectrum clear-cut and makes the choice of treatment straightforward. However, specificity can also be a limitation. Penicillinase was actually discovered and identified as a force of defense produced by the pathogen earlier than the medical application of the antibiotic itself [1]. This type of attack-and-defense relationship widely exists in nature. But again, the inappropriate and large-scale use of antibiotics during the past six decades has facilitated the evolution of resistance genes which make pathogens much more difficult to deal with. Vancomycin, widely regarded as “the last standing line against the severe infections”, has been used to treat serious MRSA infections. But resistant *S. aureus* specific to vancomycin appeared in Japan in 1997 as vancomycin-intermediate *S. aureus* (VISA) [20]

and in 2002 a higher level resistant strain was reported in Michigan, USA [21] as vancomycin-resistant *S. aureus* (VRSA). This example strongly supports the old Chinese proverb: “While the priest climbs a post, the devil climbs ten”. This war between traditional antibiotics and rapidly evolving pathogens will continue, and the later could win if antibiotics have no revolutionary step forward.

Therefore it is imperative to discover and develop antibacterial agents with novel action mechanisms to minimize the chance of drug resistance. To this end, a wide series of compounds called “antimicrobial peptides” (AMP) have been either discovered in nature or synthesized in laboratories around the world. The advent of AMPs has brought new hope to the fight against the rise of antibiotic-resistant organisms.

The earliest publication record of antimicrobial peptides can be traced back to the 1980s. Researchers injected bacteria into the pupae of the cecropia moth, and later on a 37 amino acid cationic peptide was isolated and purified from the hemolymph of the moth. Biosynthesis of this peptide was induced by the injected bacteria and the peptide showed antibacterial activity against multiple Gram-negative bacteria including *Escherichia coli* and *Pseudomonas aeruginosa* [18].

The discovery of the moth peptide was followed by another important study, in which a series of peptides were found in the granules of human and rabbit granulocytes. The molecules featured 29 to 34 amino acids, of which six cysteine residues were highly conserved and involved in intramolecular disulfide bond. Shortly after, they were found to be active against both gram-negative and gram-positive bacteria [18].

These two events are among many milestones throughout the discovery and

development history of antimicrobial peptides. Since a great number of those peptides show remarkable *in vitro* activity against bacteria with single or multiple resistances to traditional antibiotics, they possess great potential to become templates for anti-infectious drug design [19]. The common structural features of an antimicrobial peptide include positive charge and amphipathicity. They are cationic (at least 3+) due to an unusual abundance of lysine and arginine residues. Being amphipathic allows water-solubility and lipid layer-compatibility at the same time. Length ranges from 12 to 45 amino acid residues [22]. Natural occurring antimicrobial peptides generally adopt four classes of structures: α-helix, β -strand, extended coil and loop [22].

Many of those peptides can adopt different conformations when they are placed in different chemical environments and their antimicrobial activities can be correlated with the changes in conformations. The investigation of human cathelicidin LL-37 is a good example. In aqueous solutions such as phosphate buffer, circular dichroism (CD) spectroscopy shows the compound to lack secondary structure. By comparison, when in trifluoroethanol, sodium dodecyl sulphate (SDS) micelles, or phospholipid, partially or all α-helix conformation is present. Furthermore, the percentage of α-helicity is coupled to the antibacterial activity. Increased α-helical content correlates with stronger antimicrobial activities [24].

Several important characteristics of the peptide structure will affect activity and specificity, including amino acid sequence, charge density, hydrophobicity and amphipathicity. Those characteristics and their roles are listed in **table 1.1** [24].

Table 1.1: Important structural characteristics of cationic antimicrobial peptides [24]

Characteristic	Role in peptide structure and conformation
Size	12 to 45 amino acid residues in length. Should not be too short in order to adopt proper conformation; Di- and tripeptides with ntimicrobial activity have been reported.
Conformation and structure	Various conformations, but three of them are major: α-helices, relaxed coils and antiparallel β-sheet structures. Generally for natural antimicrobial peptides, amphipathic α-helical peptides are often more active than peptides with less-defined secondary structures.
Charge	Cationic due to high percentage of lysine or arginine. Highly cationic peptides are often more active than neutral peptides or those with a lower charge.
Sequence	Basic amino acid residues lysine or arginine should be included in order to keep the peptide cationic; hydrophobicity can be achieved by incorporating residues alanine, leucine, phenylalanine or tryptophan.
Hydrophobicity	Necessary for antimicrobial peptides to partition into the membrane lipid bilayer. Aromatic and hydrophobic ring in phenylalanine or tryptophan is crucial to this structural feature.
Amphipathicity	Hydrophilic residues along one side to make them water-soluble and hydrophobic residues along the opposite side to have effective interactions with lipid bilayer.

Admittedly, more-potent traditional antibiotics still serve as main-stream anti-infection

agents, but antimicrobial peptides have many intriguing advantages, including an ability to more rapidly kill target cells, unusually broad inhibitory activity spectra, activity against some of the more serious antibiotic-resistant pathogens, and a relative difficulty in selecting resistant mutation genes *in vitro*, which is vital to confront the issue of rising antibiotic-resistance [19].

1.3 Background of the Project

1.3.1 De novo Design of antimicrobial peptides incorporating unnatural amino acids

Design of new peptides from individual amino acids is a very challenging process, especially when non-RNA encoded, unnatural amino acids are present in the peptide sequence. Compared to standard organic synthesis, the design of antimicrobial peptides would be very difficult without the aid of three-dimensional physicochemical models and almost impossible starting from random design by hand [56]. Two methods can be used, at the onset of the design process: molecular modeling techniques, or adapting known naturally occurring antimicrobial peptides with well-documented structure and antibacterial activities.

Our model compound is an analog of magainin-2 amide, $Ala^{8, 13, 18}$ magainin-2 amide. It has three Ala residues at the position of 8, 13 and 18, respectively. It was chosen for its potent activity against both Gram-positive and Gram-negative bacteria and minimal interaction with mammalian cells [28]. The specificity can be explained by the difference of peptide-membrane interaction mechanisms. For eukaryotic cells, like erythrocytes, the membrane is zwitterionic. For bacterial cells, the membrane is often anionic [25]. Therefore a successful design should enable the peptide to interact effectively with anionic cell (bacteria)

membranes while zwitterionic cell membranes (mammalian animals) should stay intact [56].

In the study of Ala$^{8, 13, 18}$ magainin-2, DPC micelles and SDS micelles serve as models of zwitterionic lipids and anionic lipids, respectively [26]. Two-dimensional NMR and molecular modeling were used to investigate the interaction behavior of Ala$^{8, 13, 18}$ magainin-2 with DPC and SDS micelles. Two-dimensional NMR indicates that Ala$^{8, 13, 18}$ magainin-2 amide, when binding to DPC micelles, adopts an α-helical conformation involving residues 2–16. The four C-terminal residues converge to a loose β-turn structure. When incorporated into SDS micelles, however, Ala$^{8, 13, 18}$ magainin-2 amide adopts a β-helical conformation involving residues 7–18. The C- and N-terminal residues exhibit a great deal of conformational flexibility. Calculations were performed based on the information provided by two-dimensional NMR, generating electrostatic surface potential maps (ESP) for the different conformers of magainin-2 bound with DPC and Ala$^{8, 13, 18}$ magainin-2 bound with DPC or SDS. The results indicate that antimicrobial peptides adopt different conformations when they are bound to zwitterionic and anionic micelle models and consequently interact with the two models via different mechanisms [26]. The NMR and molecular modeling studies suggest that for any particular antimicrobial peptide, potency and selectivity are controlled by the chemical composition (zwitterionic or anionic) of the target cell's membrane [27].

Based on the studies above the design process begins with several critical factors taken into consideration, including secondary structure, molecular flexibility between regions of limited conformational flexibility, overall molecular charge distribution, charge density, and charge clusters [24]. Starting from the N-terminus, a so-called "N-capping residue" initiates

the peptide chain and this residue is usually a neutral amino acid. The 2nd residue is often a natural amino acid which is either positively charged (Arg or Lys) or hydrophobic (Phe for the most cases). This residue is critical for defining the physicochemical character of the N-terminus. The next come the 3rd and 4th residues, both of which are unnatural amino acids forming a conformationally restrained dipeptide unit. In this study the two unnatural amino acids are Tic (tetrahydroisoquinolinecarboxylic acid) and Oic (octahydroindolecarboxylic acid), respectively [56] (**Figure 1.1**). The peptide skeleton design process can be very complex but there are several key moieties to be mentioned. Spacer 1 controls the overall conformational flexibility of the molecule, which can be adjusted by arying the number of $-CH_2-$ group within; spacer 2 defines the relative distance between the peptide back bone and the membrane surface and the distance between peptide backbone and positively charged residue as well; The dipeptide unit controls local secondary structure, reduces the flexibility of the peptide backbone and induces a potential turn structure [56]. For the most cases in our peptides, the hydrophobic residue is phenylalanine or its derivatives. Assembling those elements together in a logical sequence comes up with a pool of peptides shown in **Table 1.2**. The design process does not belong to this thesis project thus it is only briefly discussed for back ground information. Frequently used unnatural amino acids are also shown in **Figure 1.1**.

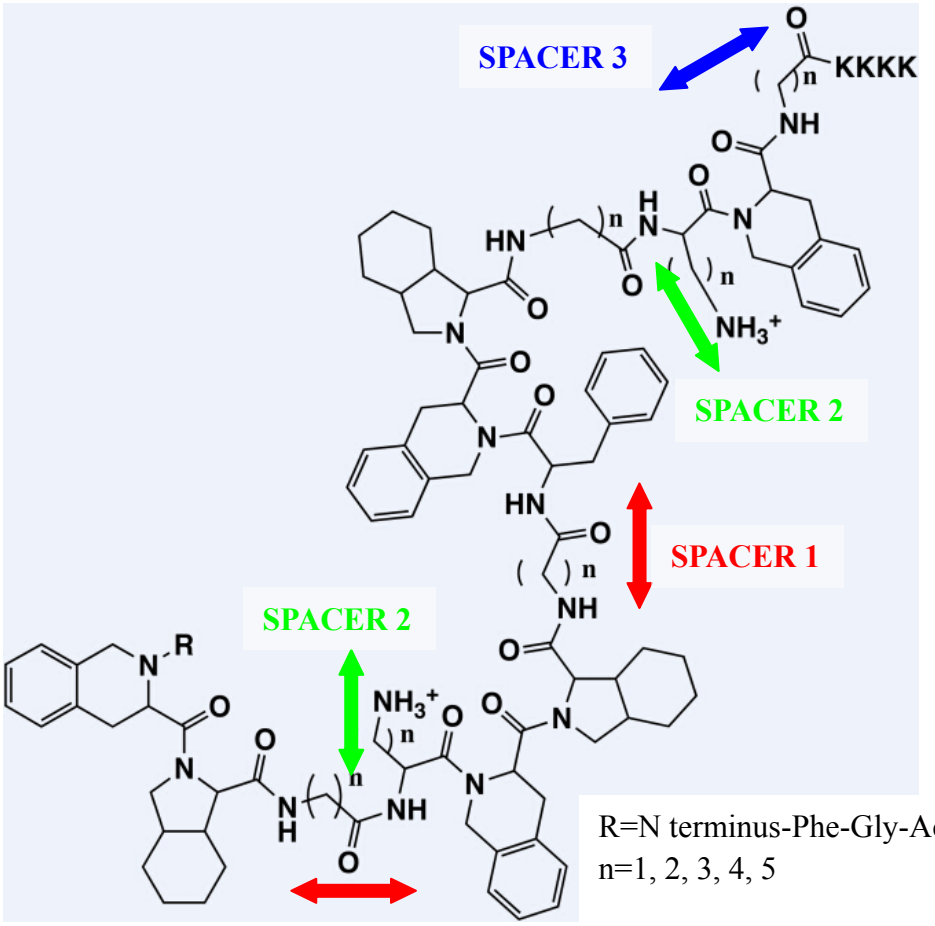

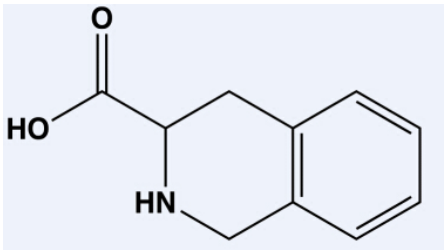

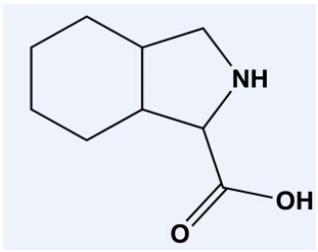

TiC (Tetrahydroisoquinoline-3-carboxylic acid) **Oic** (Octahydro-1H-isoindole-1-carboxylic acid)

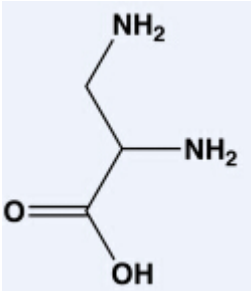

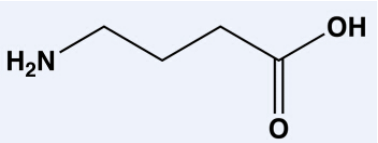

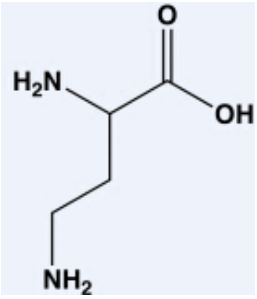

Dpr (2,3-diaminopropanoic acid) **GABA** (4-amino butyric acid) **Dab** (2,4-diaminobutanoic acid)

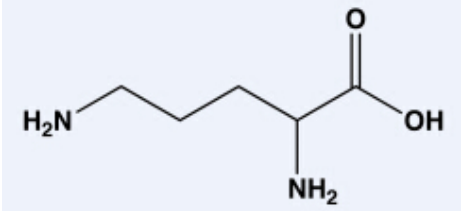

Orn (ornithine)

Figure 1.1: A basic skeleton representation of AMPs developed by Hicks et al [56] and structures of frequently used amino acids

Table 1.2: Selected novel antimicrobial peptides used in this study [5] [28]

Peptide #	Amino acid sequence
23	Ac-GF-Tic-Oic-GK-Tic-Oic-GF-Tic-Oic-GK-Tic-KKKK-$CONH_2$
29	Ac-Gaba-F-Tic-Oic-Gaba-K-Tic-Oic-Gaba-F-Tic-Oic-Gaba-K-Tic-KKKK-$CONH_2$
36	Ac-βAla-F-Tic-Oic-βAla-K-Tic-Oic-βAla-F-Tic-Oic-βAla-K-Tic-KKKK-$CONH_2$
39	Ac-GF-Tic-Oic-GK-Tic-Oic-GF-Tic-Oic-GK-Tic-KKKKK-$CONH_2$
43	Ac-GF-Tic-Oic-G-Orn-Tic-Oic-GF-Tic-Oic-G-Orn-Tic-Orn-Orn-Orn-Orn-$CONH_2$
46	Ac-βAla-Fpa-Tic-Oic-βAla-Dpr-Tic-Oic-βAla-Fpa-Tic-Oic-βAla-Dpr-Tic-Dpr-Dpr-Dpr-Dpr-$CONH_2$
53	Ac-GF-Tic-Oic-G-Dab-Tic-Oic-GF-Tic-Oic-G-Dab-Tic-Dab-Dab-Dab-Dab-$CONH_2$
56	Ac-GF-Tic-Oic-GR-Tic-Oic-GF-Tic-Oic-GR-Tic-RRRR-$CONH_2$

1.3.2 Objectives of the Project

Cell lysis mediated by an AMP is believed to occur by insertion of the AMP into the cell membrane followed by disruption of the membrane. Most structure-activity relationship studies used various zwitterionic and anionic phospholipids compositions as membrane models for bacterial membranes [29] [30]. This idea has worked well for Gram-positive bacteria which contain a single phospholipid membrane. However, this approach does not accurately model AMPs' interactions with the membranes of Gram-negative bacteria [31]. The outer membrane of Gram-negative bacteria contains a high percentage of lipopolysaccharides (LPS) on the surface of the membrane [32]. The chemical composition of LPS varies by bacteria strain and consists of three components [33]. The outer most component is the highly variable polysaccharide chain known as the O-antigen, the second component consists of the core oligosaccharide unit and the inner most component consists of the highly conserved, phospholipid-like lipid A, a polyacylated glucosamine-based bis-phospholipid [34]. LPS is highly negatively charged and functions as a semipermeable membrane that modulates the transport of AMPs across the bacteria membrane. LPS is also known as an endotoxin after release from the membrane [33]. These endotoxins are potent inducers of the innate immune system and thus cause the uncontrolled release of cytokines resulting in septic shock, leading to a series of lethal consequences including organ damage. Therefore, in the case of Gram-negative bacteria, it is of the same importance to understand the physicochemical interactions that occur between an AMP and LPS as well as the physicochemical properties of AMPs and the phospholipids components of the cell membranes in order to facilitate the new drug design of potential AMPs with remarkable

antibacterial activity against Gram-negative bacteria.

There have been previous reports on the in vitro activity of a series of synthetic AMPs that exhibited diverse inhibition activity toward *Pseudomonas aeruginosa* and *Klebsiella pneumoniae* [5]. These AMPs exhibited greater inhibitory activity against another Gram-negative bacteria Acinetobacter baumannii [5]. Therefore, the inhibitory activity of these AMPs must be defined by the interactions that occur between the AMPs and the various cell membrane components of different bacterial strains. The intent of this project is to attempt correlating the physicochemical properties of these AMPs with the binding interactions observed for a series of the membrane models of *Pseudomonas aeruginosa* and *Klebsiella pneumoniae*. From this investigation we hope to better explain the observed in vitro inhibitory activity of these AMPs and help to provide useful information on new antimicrobial drug design.

CHAPTER 2: Experimental Details.

Deuterated sodium acetate, deuterated acetic acid and LPS were purchased from Sigma Aldrich. POPC, POPG and POPE were purchased from Avanti Polar Lipids (Purity >99%). All chemicals were used without additional purification.

2.1 Sample Preparation

2.1.1 Peptide synthesis

The peptides were synthesized either by manual tBOC chemistry or by automated peptide synthesizer via FMOC chemistry [35] [36]. All peptides were purified by reverse phase HPLC using an Agilent 1100 series preparative instrument and a Vydac C18 reverse phase preparative HPLC column. Note: in this project the peptide synthesis process is not actually practiced because it's been done previously [28]. Peptide solids are used directly and this part is for background information only.

2.1.2 Preparation of mixed POPC/POPE/POPG SUVs

The appropriate amount of dry POPC, POPG and POPE was weighted out to yield a final lipid concentration of 35 mM with the desired percentage of each phospholipid. The lipid was hydrated with 2 mL of buffer (40 mM sodium phosphate, pH = 6.8) and vortexed extensively. SUVs were prepared by sonication of the milky lipid suspension using a titanium tip ultra-sonicator (Qsonica Sonicators model Q55) for approximately 40 minutes in an ice bath until the solution became transparent. The titanium debris was removed by centrifugation at 8,800 rev./min for 10 minutes using an Eppendorf table top centrifuge [37]. Final lipid concentration used for CD studies was 3.5 mM.

2.1.3 Preparation of LPS ONLY SUVs

A 4 mg sample of the appropriate lipopolysaccharide was hydrated with 4 mL of buffer (40 mM sodium phosphate, pH = 6.8) and vortexed extensively. SUVs were prepared by sonication of the milky lipid suspension using a titanium tip ultra-sonicator (Qsonica Sonicators model Q55) for approximately 10 minutes at a temperature of 40 ℃ until the solution became transparent [38]. The titanium debris was removed by centrifugation at 8800 rev/min for 10 minutes using an Eppendorf table top centrifuge.

2.1.4 Preparation of LPS-mixed phospholipid SUVs

5 mg sample of the lipopolysaccharide isolated from *Klebsiella pnemoniae* was mixed with 9.84 mg of POPC, 0.68 mg of POPG and 2.53 mg of POPE yielding a lipid composition of 75%POPC/5%POPG/20%POPE (molar ratio) or 5.07 mg sample of the lipopolysaccharide isolated from *Pseudomonas aeruginosa* was mixed with 7.66 mg of POPC, 2.79 mg of POPG and 2.52 mg of POPE yielding a lipid composition of 59% POPC/21% POPG/20% POPE each preparation was then hydrated with 2 mL of buffer (40 mM sodium phosphate, pH = 6.8) and vortexed extensively. SUVs were prepared by sonication of the milky lipid suspension using a titanium tip ultra-sonicator (Qsonica Sonicators model Q55) for approximately 40 minutes in an ice bath until the solution became transparent. The titanium debris were removed by centrifugation at 8,800 rev./min for 10 minutes using an Eppendorf table top centrifuge [37]. A similar procedure was used by Matsuzaki and co-workers to prepare LPS-POPC SUVs [39].

2.2 Circular Dichroism

The peptide solutions were prepared weighing approximately 2 mg of peptide dissolved in 1.0 mL of phosphate buffer. For LPS-lipid SUV studies 100 μL of stock peptide solution was added to 20 μL of stock LPS-lipid solution with 80 μL of phosphate buffer. For lipid SUV studies 100 μL of stock peptide solution was added to 20 μL of stock lipid solution with 80 μL of phosphate buffer. For LPS liposomes studies 350 μL of stock LPS solution was mixed with 50 μL of stock peptide solution. CD spectroscopy is very useful to monitor conformational changes in peptide. LPS can exhibit CD spectra but with careful subtraction of the LPS background meaningful spectra of the AMPs bound to the LPS can be obtained.

All CD spectra were obtained by acquiring 8 scans (accumulation) on a JASCO J-815 CD Spectrometer to achieve good S/N ratio. The signal to noise ratio (S/N) of a CD measurement is proportional to the square root of the number of scans and to the square root of the time constant [55]. Good S/N ratios can be achieved either by multiple fast scans recorded with a short time constant or by recording a small number of slow scans with a long time constant. A 0.1 mm cylindrical quartz cell (Starna Cells, Atascadero, CA) is used and a spectral width of 260 to 195 nm is selected to observe amide bond electrons absorption change [40] and thus the secondary structure change of the AMPs can be investigated. Spectra were collected using the following parameters, scan rate 20 nm/min, 1 nm bandwidth, data pitch 0.2 nm, response time 2.0 sec and 5 mdeg sensitivity at room temperature. The spectral bandwidth is generally set to 1 nm. The data pitch determines the number of data points taken during the scan, i.e., number of data points per nm, will not directly influence the noise level. However if post run data processing will be applied to reduce the noise, it's

recommended to collect as many data points as possible to increase the efficiency of the post run filtering algorithm [55]. Response time is also known as data integration time, which is generally 2 seconds. The product of scanning speed (20 nm/min) and response time (2.0 sec) should be less than 60 $nm \cdot min^{-1} \cdot sec$ [55]. If higher values are used there will be significant errors in both the positions and intensities of the observed CD bands.

Contributions due to liposomes or LPS were eliminated by subtracting the lipid or LPS spectra of the corresponding peptide-free solutions. All analysis of CD spectra will be conducted after smoothing (Gaussian function) using the JASCO Spectra Analysis program [40]. CD spectra that exhibited HT values of greater than 500 volt (V) (or 600 V for a less strict standard) will not be used because CD spectra will be seriously distorted if the photomultiplier voltage rises above this limit.

CHAPTER 3: Results and Discussions

3.1 Circular Dichroism (CD) Studies of AMPs Interacting with Three Liposome Systems

3.1.1 Liposome System One: Lipopolysaccharide (LPS) Outer Membrane isolated from Gram-negative Bacteria *Pseudomonas aeruginosa* and *Klebsiella pneumoniae*

From outermost to innermost there are three main components in the LPS monomer are the O-antigen, inner core oligosaccharide, and the phospholipid-like lipid A. The O-antigen is the most variable domain of LPS and the sugar moiety among different bacterial species. For instance, over 160 different O-antigen structures have been identified from different *E. coli* strains [33]. The core oligosaccharide is the first component outside the cell membrane between the O-antigen and lipid A and its sugar moiety is less variable than O-antigen. The core oligosaccharide usually contains sugars such as heptose and 3-deoxy-D-mannooctulosonic acid (aka KDO, keto-deoxyoctulosonate). The KDOs are often phosphorylated. These KDOs and heptoses make up the "inner core" section [41]. The lipid A portion, from which the LPS molecule actually “grows” and projects from cell membrane, is the most conserved section within Gram-negative bacteria outer membrane structure. Chemically it consists of a glucosamine disaccharide unit which is phosphorylated and tailed with many kinds of fatty acids [43] [44]. A great portion of the toxicity of Gram-negative bacteria comes from the lipid A, since when bacterial cells are lysed by the immune system, fragments of membrane containing lipid A are released into the circulation, causing well-known fatal endotoxic shock (also called septic shock) [42].

Unlike phospholipids, LPS has a significant negative single peak in CD spectra around 185 to 200 nm due to the oligosaccharide headgroup [38]. The absorption wavelength

depends on the chemical composition of different bacterial strains. Therefore, for each distinct peptide-LPS CD study, preparation of pure LPS with the identical amount of lipid in buffer is necessary so that the LPS background signals can be subtracted in order to compare the conformational change of the peptide upon interacting with LPS liposomes [38].

In the infection process, outer membrane LPS tends to form vesicles, which in complex fluids may resemble the physiological and chemical characteristics of the original bacterium [45]. Since the infection occurs under physiological conditions within host tissues, and Lipid A has a large amount of acyl chains just like other common phospholipids, it is logical for us to assume that under the experimental condition of LPS solution preparation previously mentioned, LPS from *Pseudomonas aeruginosa* and *Klebsiella pneumoniae* can form similar vesicles which resembles the natural outer membrane.

Since LPS is the first barrier that peptide molecules should contact with and migrate through when they interact with Gram-negative bacteria cell membrane [33], it is necessary to investigate the interaction between the peptide and the pure LPS and CD is a useful tool to monitor conformational changes of peptide from peptide alone in phosphate buffer and peptide-LPS complex. As previously stated in the experimental section, LPS liposome stock solution was prepared by extensive vortex and sonication in phosphate buffer according to the work by Brandenburg K. et al and it is believed that after vortex and sonication LPS may form multilayer vesicles [54], however, it is yet to be confirmed. For our project, though it still remains unclear what kind of vesicle the LPS may form under the said experimental condition, it's still useful for providing a model system to study peptide-LPS interaction by CD spectroscopy.

Table 3.1: Lipopolysaccharides (LPS) and phospholipid compositions of the SUVs used in this project

Model #	Bacteria Strain	Region of Membrane	composition	Abbreviation
1	*Klebsiella pneumoniae*	outer leaflet of outer membrane	100% LPS	LPS (K)
2	*Pseudomonas aeruginosa*	outer leaflet of outer membrane	100% LPS	LPS (K)
3	*Klebsiella pneumoniae*	outer membrane (complete)	LPS /75% POPC/20%POPE/5% POPG	LPS (K)-mix (K)
4	*Pseudomonas aeruginosa*	outer membrane (complete)	LPS/59% POPC/20% POPE/21% POPG	LPS (P)-mix (P)
5	*Klebsiella pneumoniae*	inner membrane	75% POPC/20% POPE/5% POPG	Mix (K)
6	*Pseudomonas aeruginosa*	inner membrane	59% POPC/20% POPE/21% POPG	Mix (P)

CD spectra of pure LPS and peptide (binding with LPS, LPS spectrum subtracted)

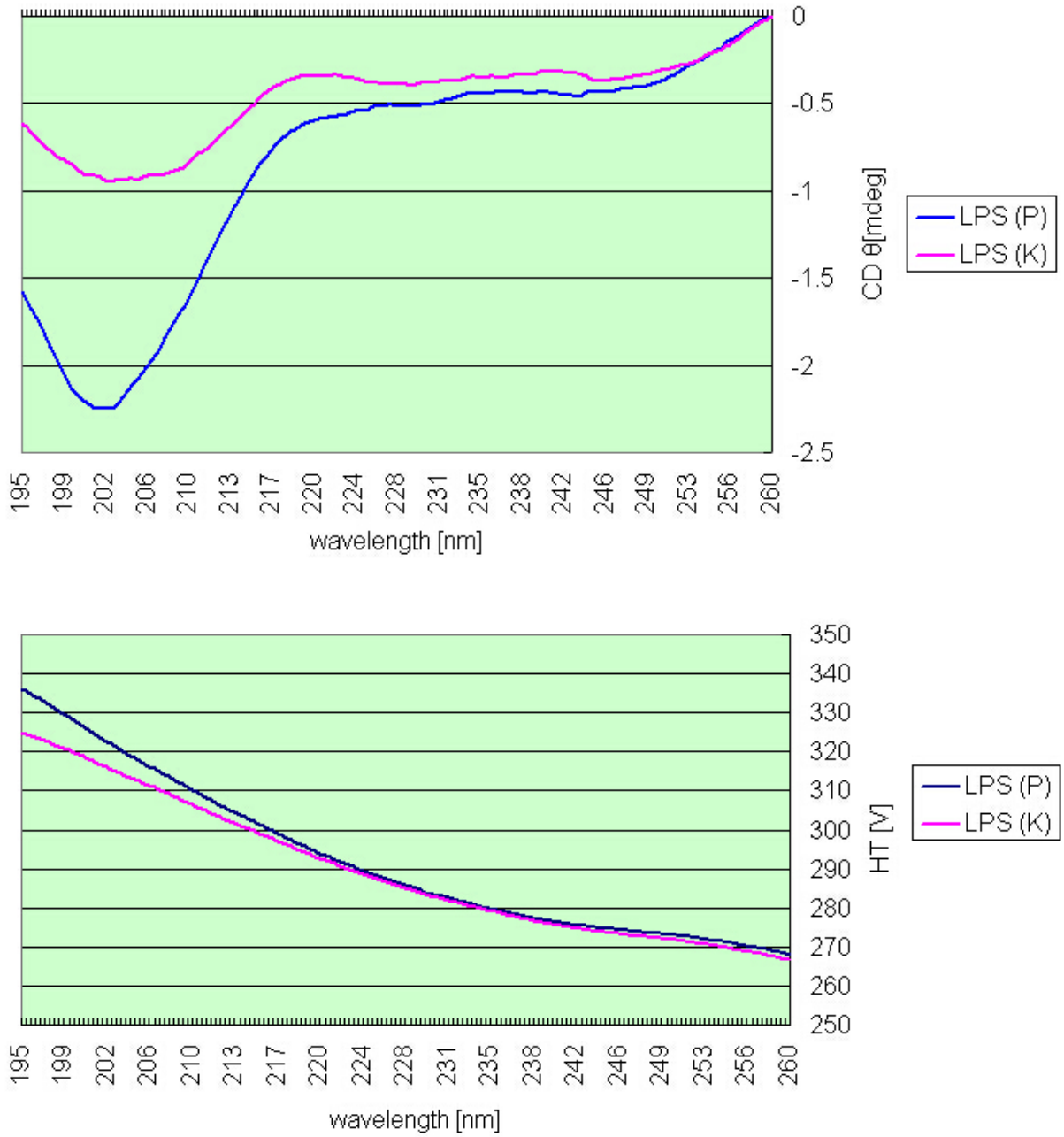

Figure 3.1: (Top) CD spectra of **LPS vesicle alone** from *Pseudomonas aeruginosa* (P) and *Klebsiella pneumoniae* (K) in phosphate buffer, where the buffer baseline has been subtracted from the original spectrum. Since the molecular weight of LPS varies from different bacteria strains and can not be estimated, molar ellipticity [θ] is not able to be calculated and the original CD absorption in mdeg is used as the Y-axis. (Bottom). Corresponding HT value (in

Volt) curve of LPS (P) and LPS (K) alone as plotted against wavelength in [nm]. Generally HT values which go beyond 500 V are unacceptable.

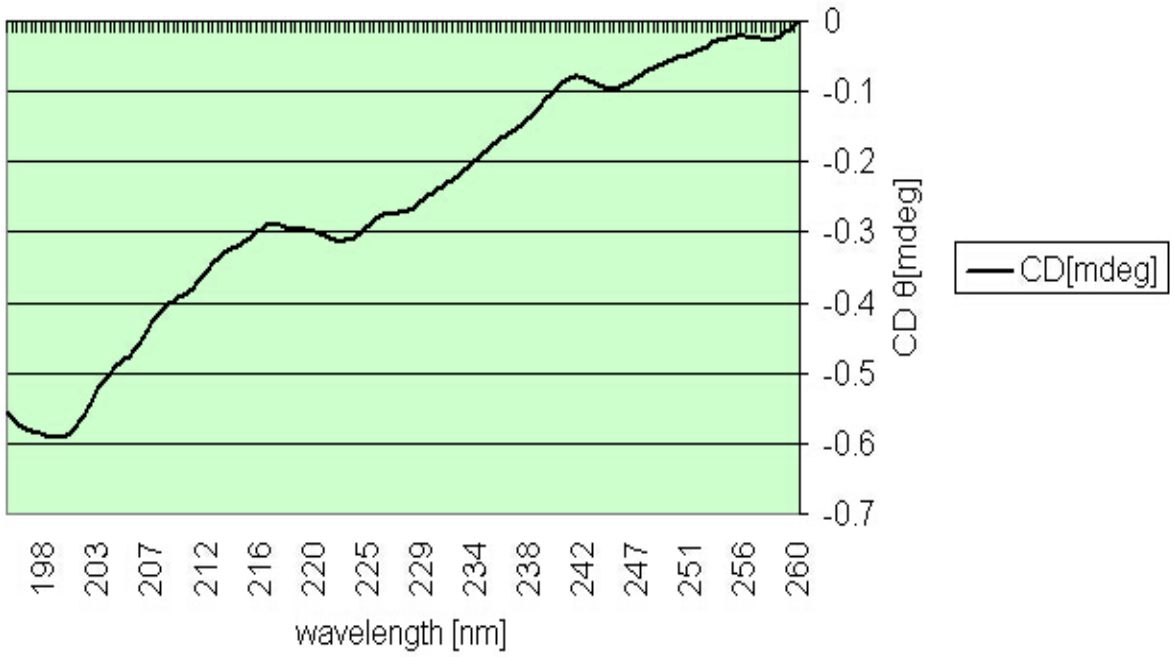

Figure 3.2: CD spectrum of buffer (50 mM sodium phosphate, pH = 6.8)

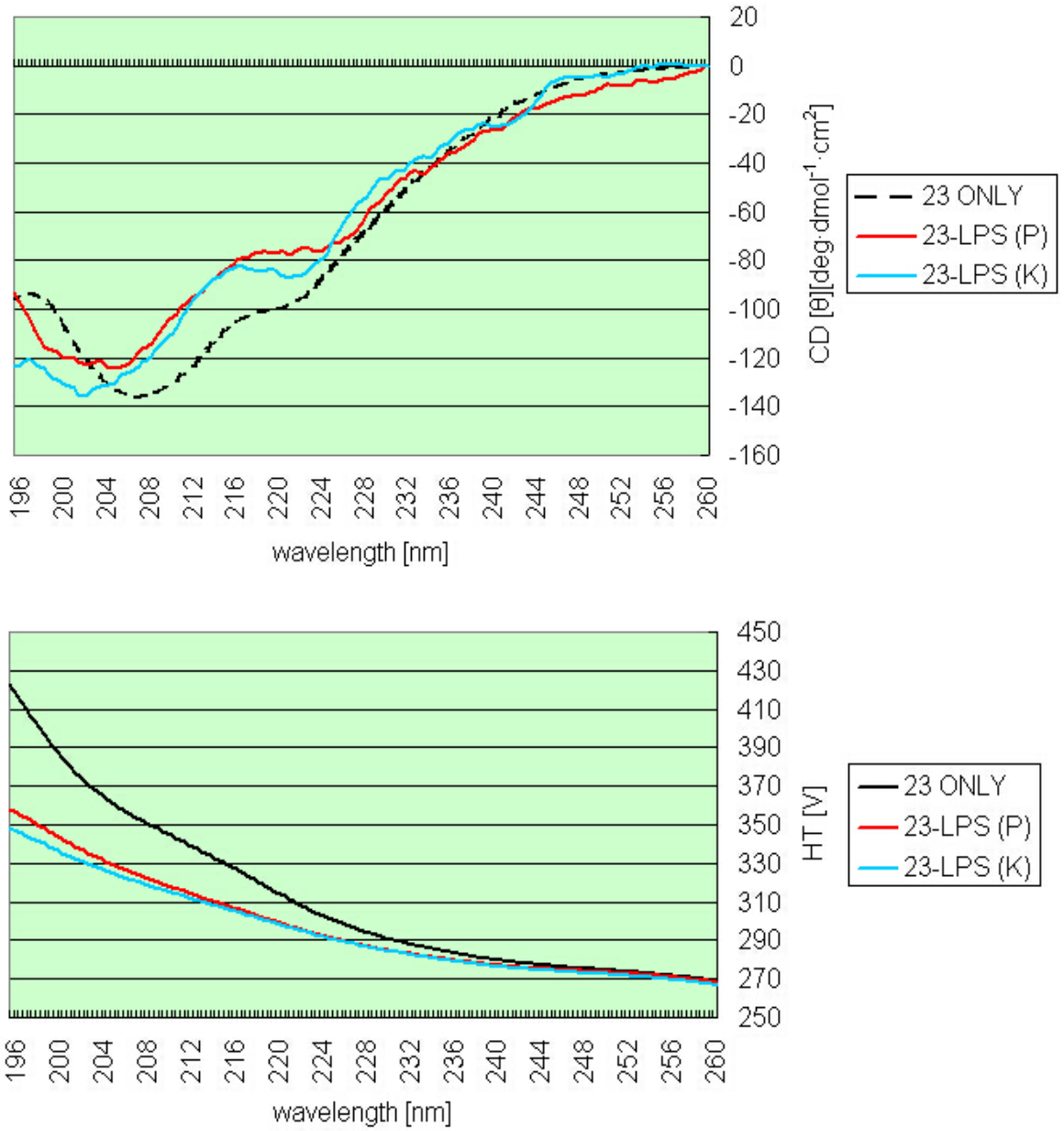

Figure 3.3: (Top) CD spectra of peptide **23** alone (dashed line, **black**), peptide **23** with LPS vesicle from *Pseudomonas aeruginosa* (P) (solid line, **red**) and *Klebsiella pneumoniae* (K) (solid line **blue**) in phosphate buffer converted into molar ellipticity [θ], where the buffer baseline has been subtracted from the original spectrum of peptide alone, and the LPS signal has been subtracted from original peptide-LPS complex signal. Thus all three spectra shown at top represent peptide CD signals in different chemical environments. (Bottom) corresponding HT values which go beyond 500 V are unacceptable.

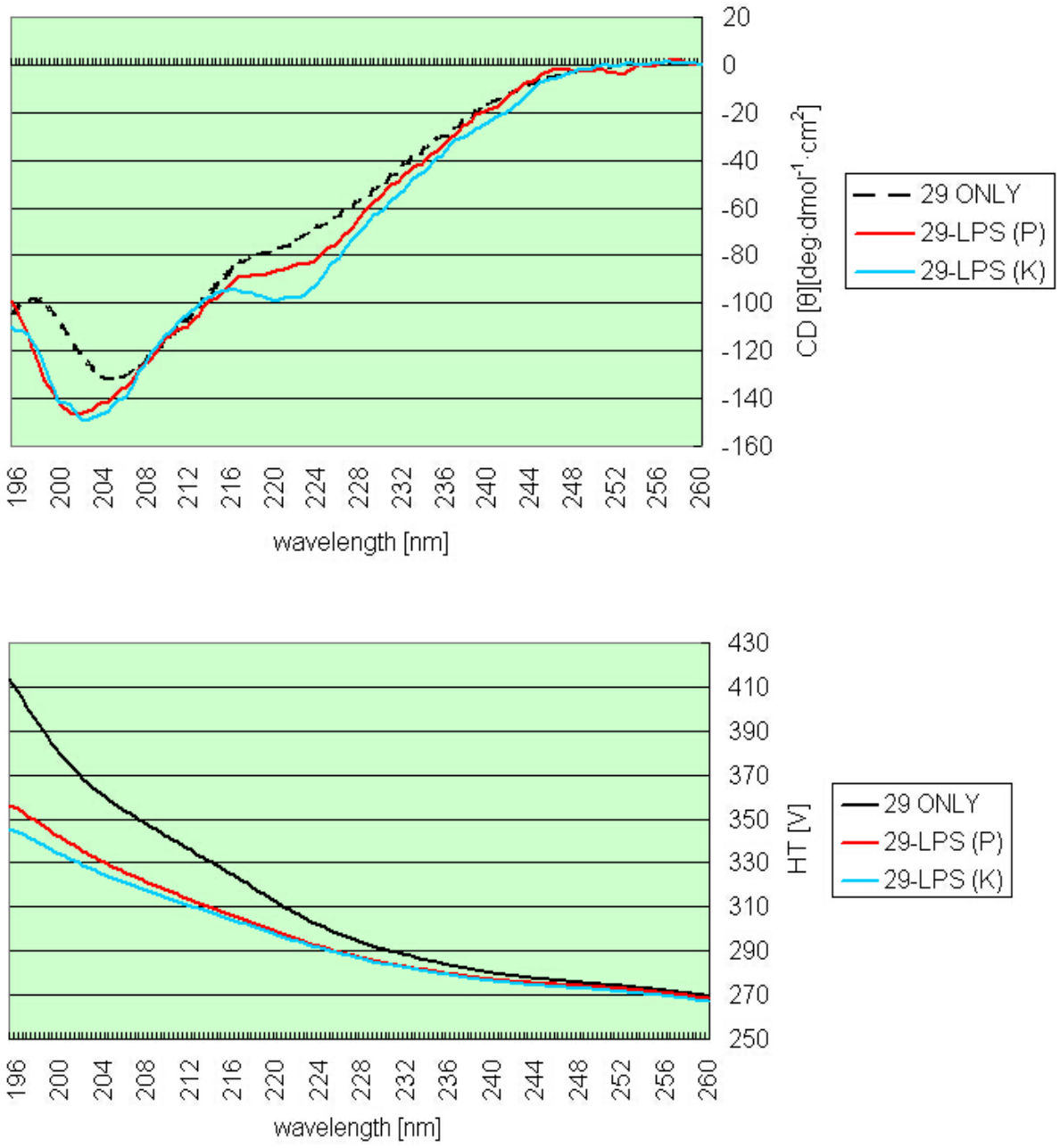

Figure 3.4: CD spectra of peptide **29** alone (dashed line, **black**), peptide **29** with LPS vesicle from *Pseudomonas aeruginosa* (P) (solid line, **red**) and *Klebsiella pneumoniae* (K) (solid line **blue**) in phosphate buffer converted into molar ellipticity [θ], where the buffer baseline has been subtracted from the original spectrum of peptide alone, and the LPS signal has been subtracted from original peptide-LPS complex signal. Thus all three spectra shown at top represent peptide CD signals in different chemical environments.

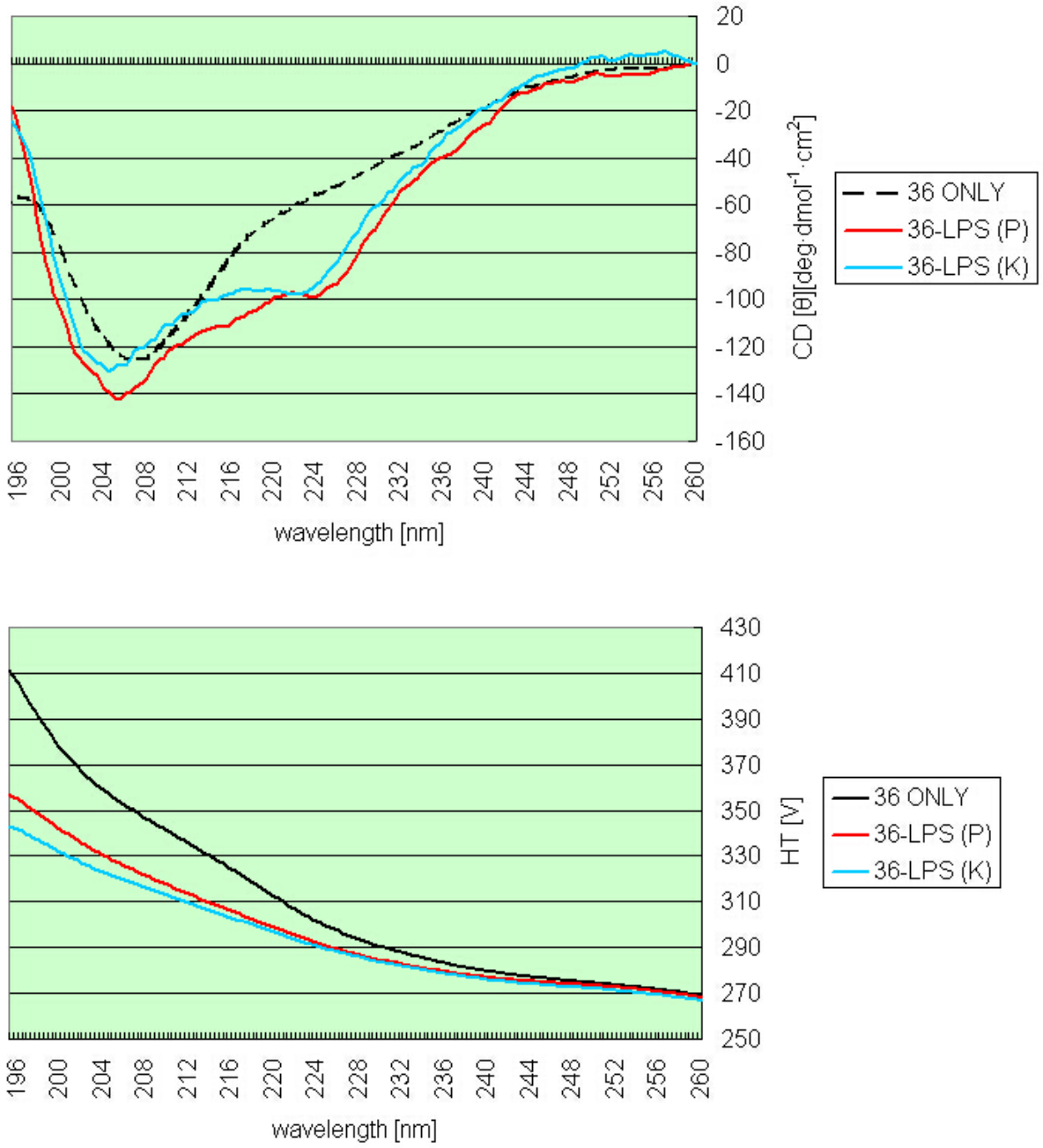

Figure 3.5: CD spectra of peptide **36** alone (dashed line, **black**), peptide **36** with LPS vesicle from *Pseudomonas aeruginosa* (P) (solid line, **red**) and *Klebsiella pneumoniae* (K) (solid line **blue**) in phosphate buffer converted into molar ellipticity [θ], where the buffer baseline has been subtracted from the original spectrum of peptide alone, and the LPS signal has been subtracted from original peptide-LPS complex signal. Thus all three spectra shown at top represent peptide CD signals in different chemical environments.

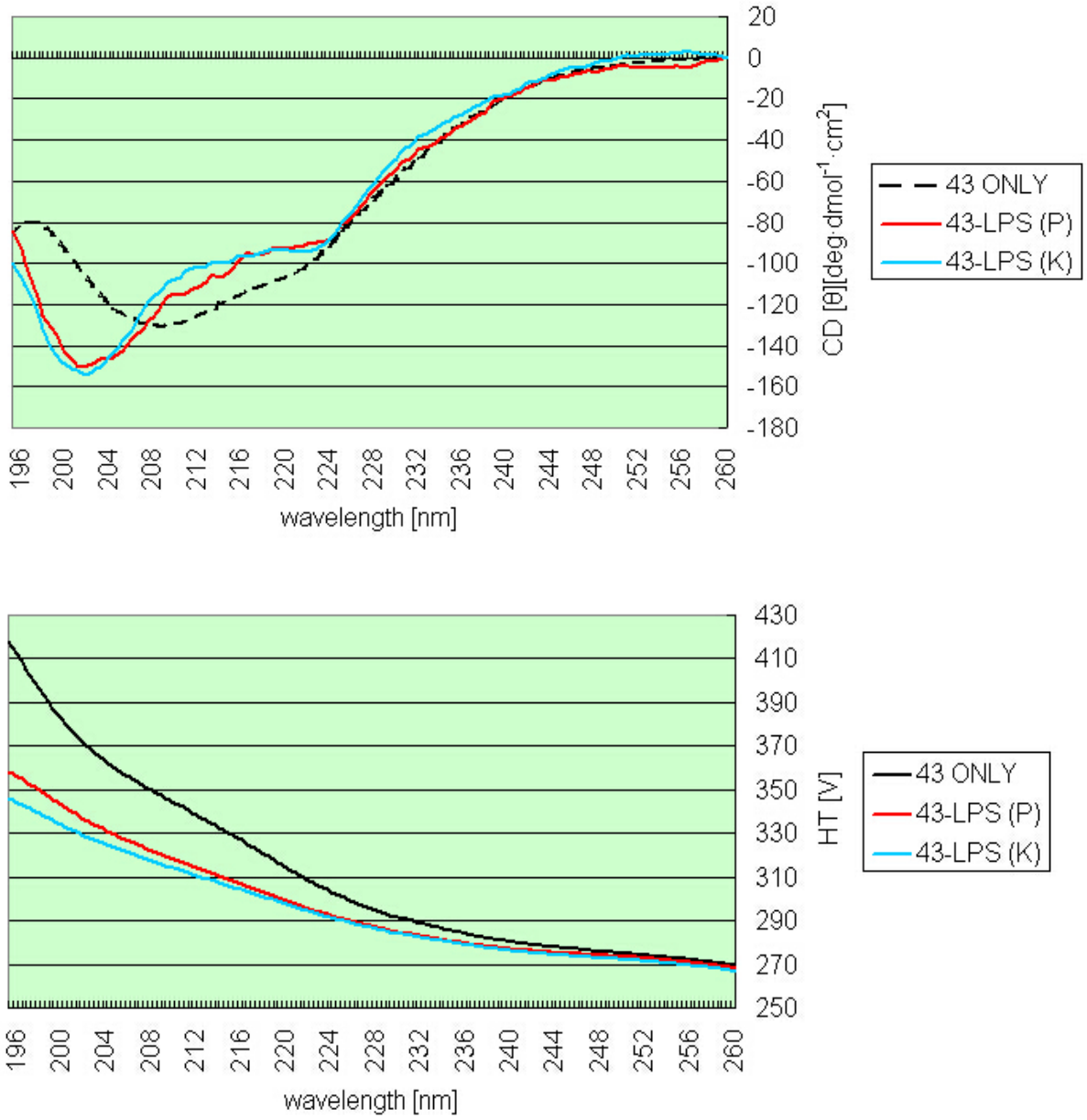

Figure 3.6: CD spectra of peptide **43** alone (dashed line, **black**), peptide **43** with LPS vesicle from *Pseudomonas aeruginosa* (P) (solid line, **red**) and *Klebsiella pneumoniae* (K) (solid line **blue**) in phosphate buffer converted into molar ellipticity [θ], where the buffer baseline has been subtracted from the original spectrum of peptide alone, and the LPS signal has been subtracted from original peptide-LPS complex signal. Thus all three spectra shown at top represent peptide CD signals in different chemical environments.

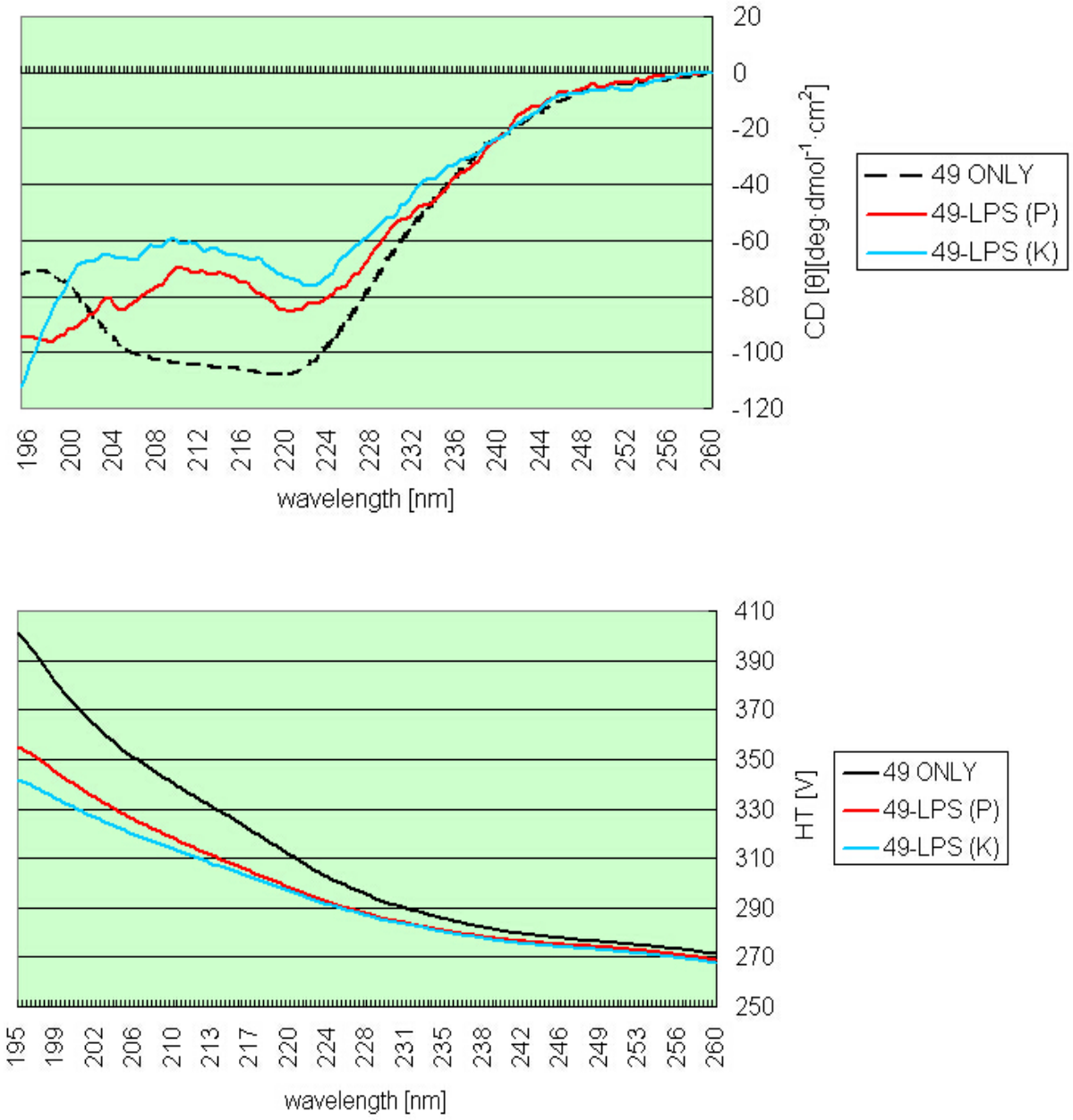

Figure 3.7: CD spectra of peptide **49** alone (dashed line, **black**), peptide **49** with LPS vesicle from *Pseudomonas aeruginosa* (P) (solid line, **red**) and *Klebsiella pneumoniae* (K) (solid line **blue**) in phosphate buffer converted into molar ellipticity [θ], where the buffer baseline has been subtracted from the original spectrum of peptide alone, and the LPS signal has been subtracted from original peptide-LPS complex signal. Thus all three spectra shown at top represent peptide CD signals in different chemical environments.

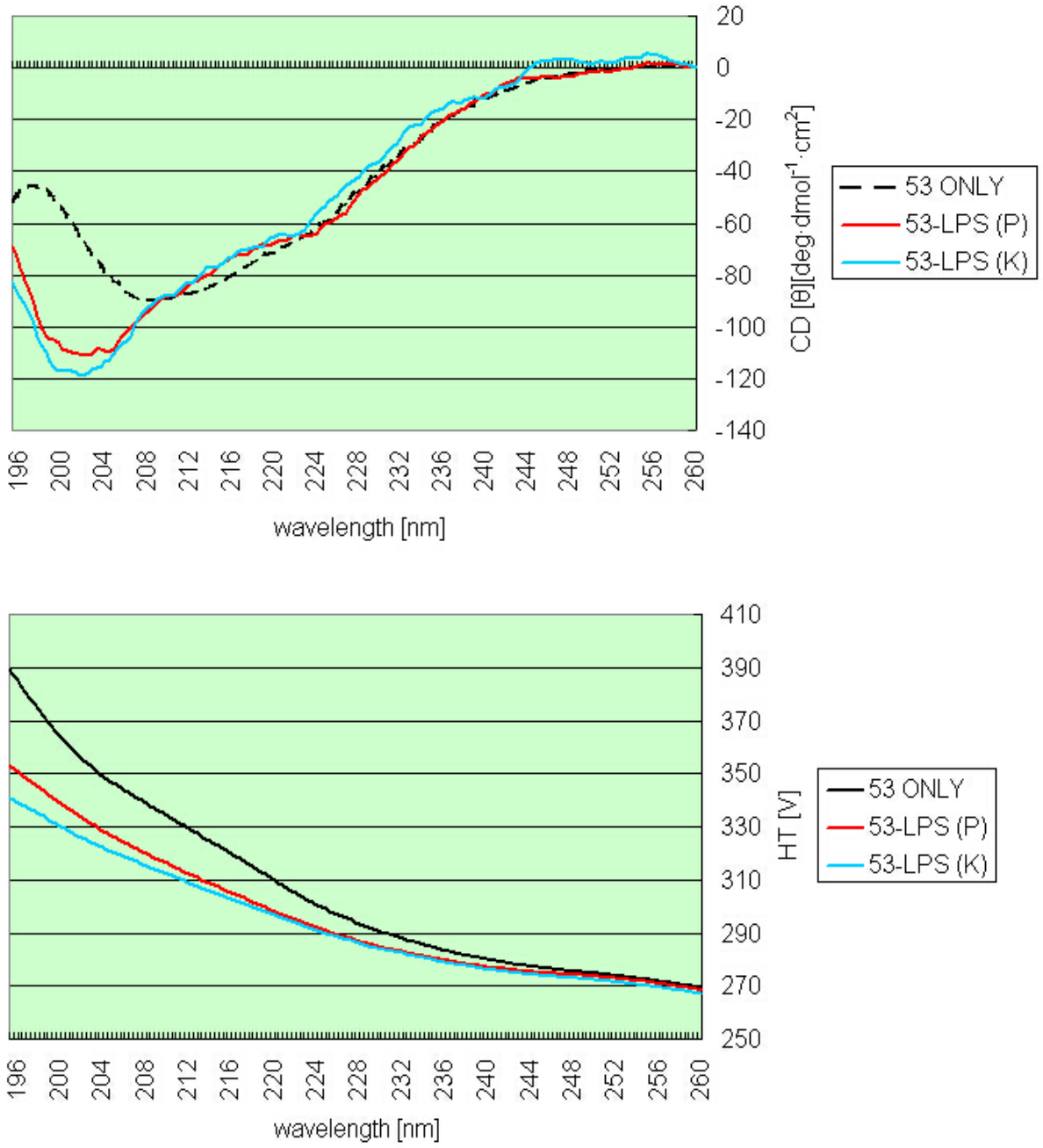

Figure 3.8: CD spectra of peptide **53** alone (dashed line, **black**), peptide **53** with LPS vesicle from *Pseudomonas aeruginosa* (P) (solid line, **red**) and *Klebsiella pneumoniae* (K) (solid line **blue**) in phosphate buffer converted into molar ellipticity [θ], where the buffer baseline has been subtracted from the original spectrum of peptide alone, and the LPS signal has been subtracted from original peptide-LPS complex signal. Thus all three spectra shown at top represent peptide CD signals in different chemical environments.

Discussion of CD spectra of peptide-LPS interaction

The y-axis unit of each set of the peptide alone and peptide-LPS (LPS subtracted) spectra has been converted into molar ellipticity [θ] from the original raw ellipticity θ data in millidegree; the advantage of using molar ellipticity is that it eliminates the concentration variance brought about by using different batches of peptide stock solutions. Thus it is more rigorous to compare spectral differences between the peptide alone and peptide-LPS. All the spectra shown above are on the same scale and the change of the peptide conformation can be observed and investigated.

Inspection of each peptide's CD spectra shows that, firstly, the peptide conformation has changed upon mixing with LPS vesicles, from its native conformation in phosphate buffer, indicating peptide molecules indeed interact with LPS. This conformation change is presented through the shifts of the absorption wavelength and change of the CD intensity at the minima. Secondly, each peptide interacts with LPS from *Pseudomonas aeruginosa* (P) and *Klebsiella pneumoniae* (K) in a similar manner, which is supported by the fact that the shape, intensity, and position of the absorptions with LPS (P) and LPS (K) are very similar. It can be inferred that even though the two LPS species are very different in terms of specific sugar moiety sequence and lipid A chemical composition [46] [47], the peptide can not discriminate such variance and interacts with the two LPS species as if they are the same. At the same time, different peptides shows totally different spectra when interacting with the same LPS (P) or LPS (K). This shows it is the physicochemical properties of peptide and LPS, such as hydrophobicity and net surface charge, that determine the interaction behavior and thus the overall CD spectra shape of the peptides.

What follows are qualitative discussions of conformational changes of each peptide shown by each set of CD spectra above:

(1) Peptide **23** (**Figure 3.3**): The peptide spectrum shows negative bands at ~207 nm. By comparison, when LPS (P or K) is mixed with the peptide, absorption of the 207 nm band shifts to approximately 202 nm. The shoulder (~220-224 nm) shifts to longer wavelength ~224-228 nm in the presence of LPS. This result indicates peptide **23** conformation changes compared with the original conformation. However, the percentage of original conformation change can not be estimated because of the introduction of the unnatural amino acids.

(2) Peptide **29** (**Figure 3.4**): The peptide alone has an intense band at ~205 nm and shows a very weak shoulder at ~216 nm. When mixed with LPS, the intense band shifts to approximately 202 nm. Meanwhile, the shoulder remains at ~222 nm. This indicates peptide **29** adopts a conformation which is different from that of peptide alone when LPS is added.

(3) Peptide **36** (**Figure 3.5**): This peptide has a very similar binding trend to that seen with peptide **29**. The shoulder at ~218 nm begins to show up when LPS is added, leading to an indication of conformation change.

(4) Peptide **43** (**Figure 3.6**): Again, the 222 nm shoulder becomes apparent and the minimum at 209 nm is blue-shifted to ~203 nm, a case which is just similar with peptide **23**, **29** and **36**. Presumably it adopts a different conformation compared with the original conformation.

(5) Peptide **46**: the CD spectra of peptide with LPS are very weak and noisy and it's difficult to see any conformational features. Thus spectra of peptide **46** are not shown.

(6) Peptide **49** (**Figure 3.7**): Spectrum feature change is very similar to that of peptide **29**, along with dramatic conformation change from the peptide alone. Once mixed with LPS

(either P or K), the negative peak at ~222 nm changes, at the same time a negative band around 195 nm appears in peptide-LPS spectra, indicating a dramatic conformational change.

(7) Peptide **53** (**Figure 3.8**): The negative peak at ~207 nm of the peptide shifts to ~202 nm. One very tiny shoulder begins to show up around 225 nm, otherwise the trend of conformational change is still similar to peptide **23**, **29**, **36** and **43**. But compared with other peptides that show a very significant change in the 225 nm band, peptide **53** shoulder change is hardly observable.

(8) Peptide **56**: the CD spectra of peptide with LPS are very weak and noisy and it's difficult to see any conformational features. Thus spectra of peptide **56** are not shown.

From the above, it can be concluded that different peptide residue sequences decide the difference of the physicochemical properties of the peptides. As a result, the CD spectra of peptides interacting with LPS vesicles also become different in terms of the shapes and intensities. The main objective of this project is to qualitatively correlate the CD spectral features of peptides with the physicochemical properties of peptides in an effort to further understand structure-activity relationships.

As previously mentioned in Chapter One, the peptides used in this project consist of four key components: Tic-Oic dipeptide units, which reduce the overall peptide molecular flexibility; SPACER # 1, which defines the distance between the two Tic-Oic dipeptide units. (They are Glysine (G), β-Alanine (β-Ala) and GABA (γ-aminobutyric acid) for the eight peptides discussed above); SPACER # 2, which defines the distance between the peptide backbone and the positively charged side chain nitrogen atom as well as determining the overall charge density of the molecule. (These include Lysine (K), 2,3-diaminopropionic acid

(Dpr), 2,4-diaminobutanoic acid (Dab) and 2,5-diamino-pentanoic acid (Orn)); and finally amino acids with hydrophobic side chains, which are also substantial to give peptides the appropriate level of hydrophobicity that is important for peptide interacting with hydrophobic components of various liposomes, including both LPS and phospholipids. Such hydrophobic side chain species can be Phenylalanine (F), 4-fluorophenylalanine (Fpa) and 4-Nitrophenylalanine (Nph). It can be expected that the interaction between peptides and LPS vesicles is a combined result of physicochemical properties of the four key components.

Since the four key components are all variables which determine peptides' physicochemical properties, it makes the comparative study much easier and more straightforward if all these variables are collected in a table so that we can simply focus on those important modules rather than reading through long peptide sequences.

Table 3.2: SPACER #1, SPACER # 2, and hydrophobic residues for each peptide [5].

Peptide Number #	Spacer # 1	Spacer #2	Hydrophobic
23	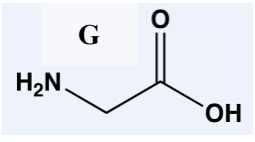	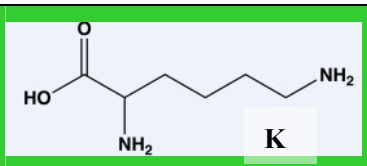 **K**	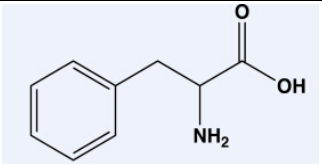 **F**
29	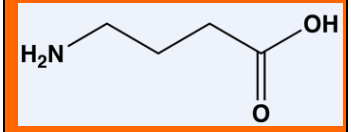 **GABA**	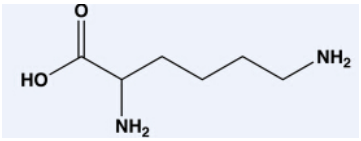	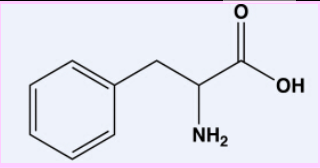

36	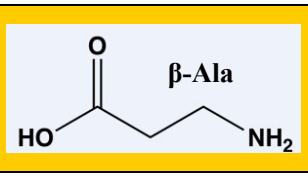	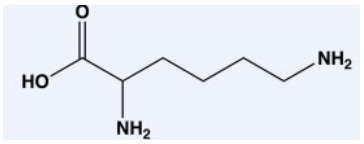	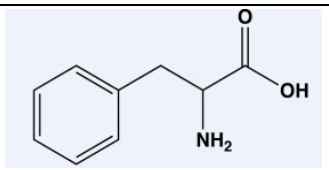
43	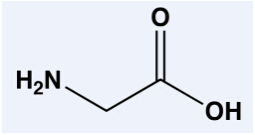	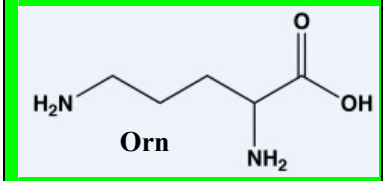	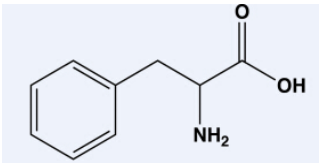
46	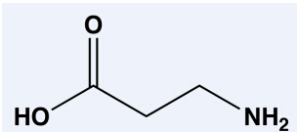	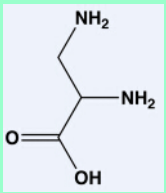	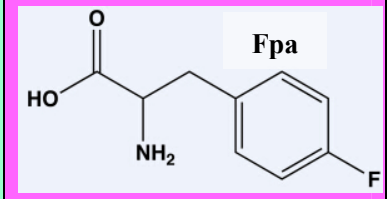
49	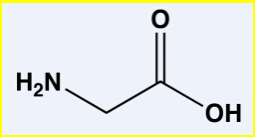	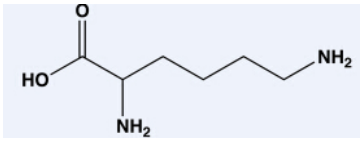	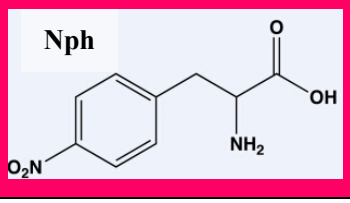
53	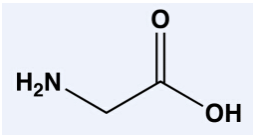	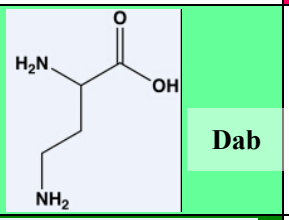	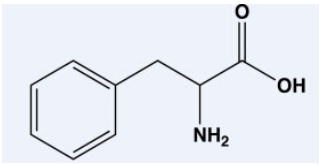
56	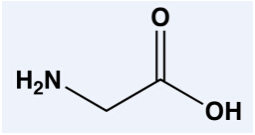	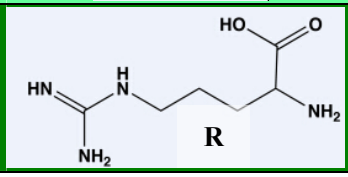	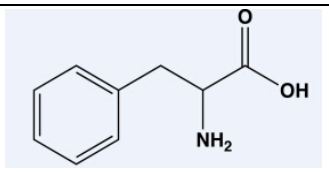

For the columns of SPACER #1 and SPACER # 2, lighter color indicates shorter carbon chains and darker color indicates longer. Thus for SPACER #1 the length of Gly＜β-Ala＜GABA; for SPACER # 2 Dpr＜Dab＜Orn＜K. Arginine (R) is not in the comparison sequence for its special complex guanidinium distal end. For the column of hydrophobic residues, the pink color scale shows the substitution variance of p-substituted phenylalanine, from natural phenylalanine (F) to 4-Nitrophenylalanine (Nph).

There are two important comparison groups in this part of investigation. One group

includes **23**, **29** and **36**, which studies the effect of the length of the SPACER # 1, the other group includes **23**, **43** and **53** to focus on SPACER # 2. Both groups keep the other variables constant.

Peptide Number #	Spacer # 1	Spacer #2	Hydrophobic
23	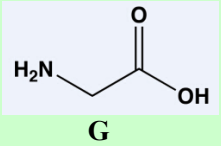 G	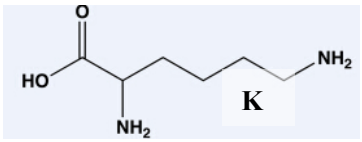 K	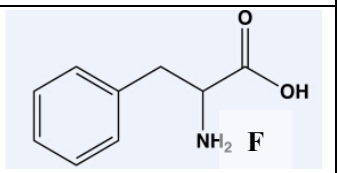 F
36	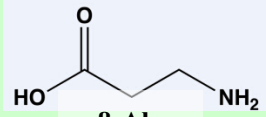 β-Ala	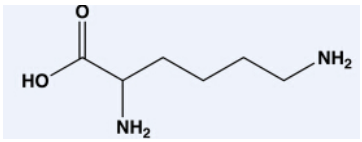	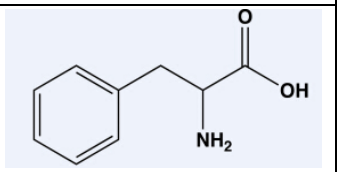
29	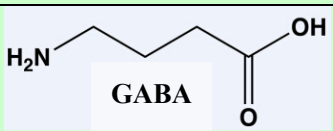 GABA	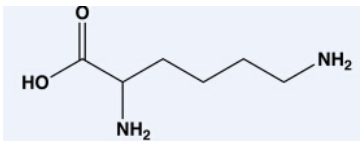	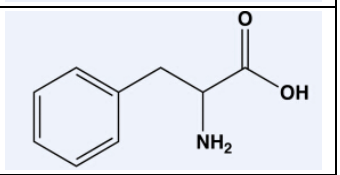

Table 3.3: Structural feature comparison of peptide # 23, # 36 and # 29

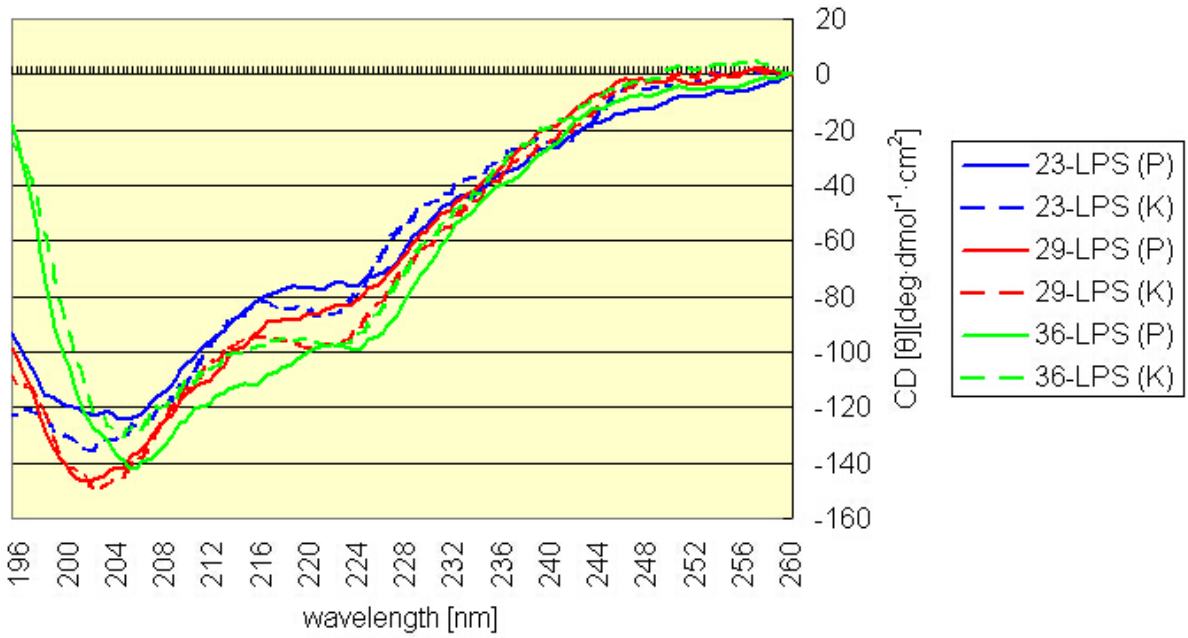

Figure 3.9 CD spectra comparison of peptide **23**, **29** and **36** with LPS (P) and (K)

The only variable among this group is the length of SPACER # 1 side chain, which is Glycine for **23**, β-alanine for **36** and GABA for **29**, respectively, and the length has been put in ascending order. The three residues here are very similar in chemical property except for small changes of hydrophobicity due to the different number of side chain $–CH_2-$ groups. All three peptides show negative shoulder minima at ~225 nm. The first minima of **23** and **29** are at shorter wavelength at ~ 203 nm compared with that of **36** at ~ 207 nm. Though not so dramatic, there is a positive correlation between the length of SPACER # 1 and the spectra shape at the first negative minima, indicating that as the length of SPACER # 1 increases, the peptide conformational flexibility possibly becomes higher and conformational change is more significant upon biding with LPS.

The other comparison group includes **23**, **43** and **53**, focusing on SPACER # 2 variation, is shown below:

Peptide Number #	Spacer # 1	Spacer #2	Hydrophobic
53	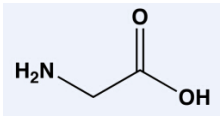 **G**	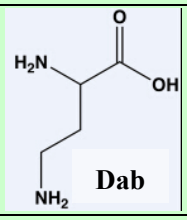 **Dab**	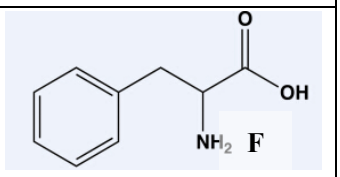 **F**
43	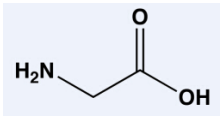	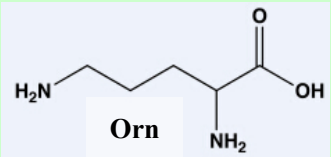 **Orn**	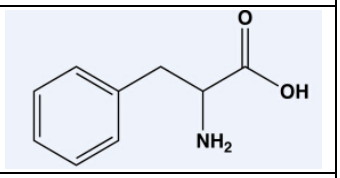
23	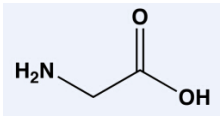	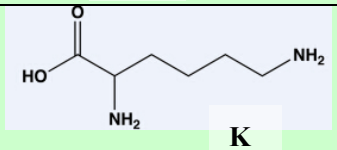 **K**	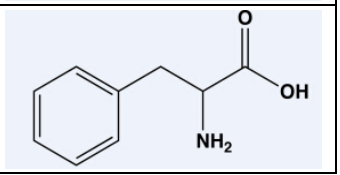

Table 3.4: Structural feature comparison of peptide # 23, # 43 and # 53

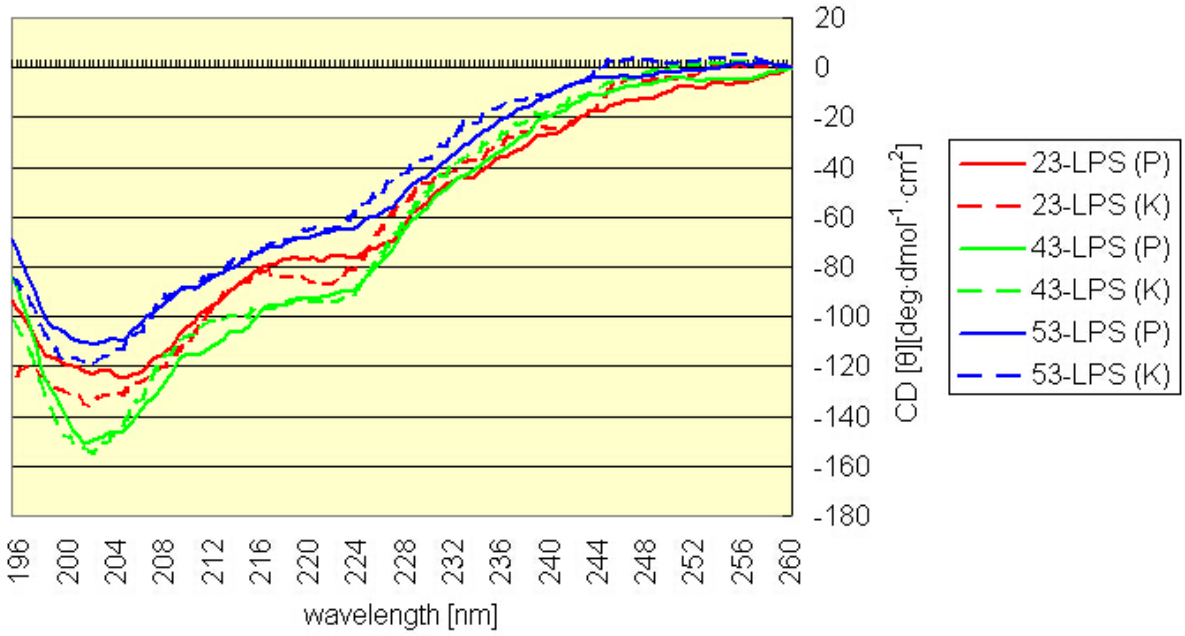

Figure 3.10 CD spectra comparison of peptide **23**, **43** and **53** with LPS (P) and (K)

Peptide # 53 has the shortest SPACER # 2 side chain among the three. An interesting observation is that the CD spectra of # 23 and **43** both show second negative minima at ~ 225 nm but **53** almost does not show such a minimum, which at least indicates that **23** and **43** adopt different conformation compared with **53**. However, with careful inspection of the spectra comparison, the correlation between SPACER # 2 side chain length and CD spectra minima feature is not so immediately intuitive. Thus the hydrophobicity (shown in table 7) of SPACER # 2 side chain must be considered as an important factor along with side chain length. Side chain of **53** is 2,4-diaminobutanoic acid (Dab) and it's the shortest side chain among the three, the hydrophobicity is medium, thus the effect of side chain length overweighs hydrophobicity and **53** shows the least conformation flexibility upon binding with LPS. Peptide **23** has the longest side chain and highest hydrophobicity at the same time, thus the net effect of the two factors balances out and the spectrum lies between **43** and **53**. With the similar consideration, peptide **43** has the most molecular flexibility among the three.

In summary, the net effect of SPACER # 2 side chain is complicated, the delocalization of positive charge and hydrophobicity balance mutually to determine the interaction between peptides and LPS.

Table 3.5: The combined Consensus Scale (CCS) (hydrophobicity) (the 4th column)

Amino acid	Number of Carbons in side chain	Distance (in Å)	Hydrophobicity	Total Hydrophobicity in peptide
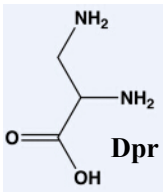	1	2.56	-9.3	-55.8
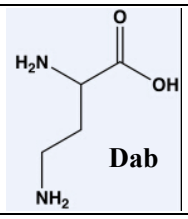	2	3.9	-9.5	-57.0
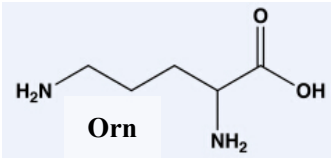	3	5.0	-9.0	-54.0
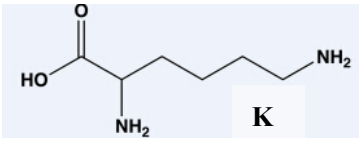	4	6.4	-9.9	-59.4
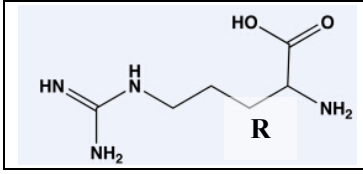	3	7.0	-10.0	-60.0

Therefore it is not one single factor that determines the binding property of the peptides with LPS, but instead it's a result of a combination of factors. There are always at least three important factors that control the binding interactions between peptides and membrane models: (1) positive charge distribution of SPACER # 2 side chain, (2) overall molecular

hydrophobicity and (3) molecular flexibility of the peptide backbone which is primarily controlled by the physicochemical property of SPACER # 1.

Lastly, peptide **49** is relatively special in terms of CD spectra shape so it's difficult to place it into any group and make comparisons. The only possible comparison is with peptide **23**, in which the only variable is the hydrophobic residue, a 4-Nitrophenylalanine (Nph).

Peptide Number #	Spacer # 1	Spacer #2	Hydrophobic
23	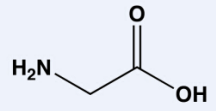	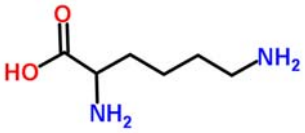	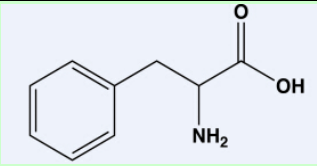
49	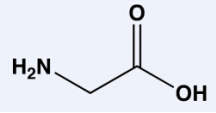	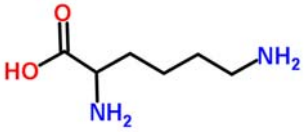	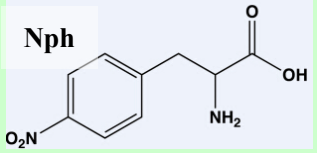

Table 3.6: Structural feature comparison of peptide # 23 and # 49

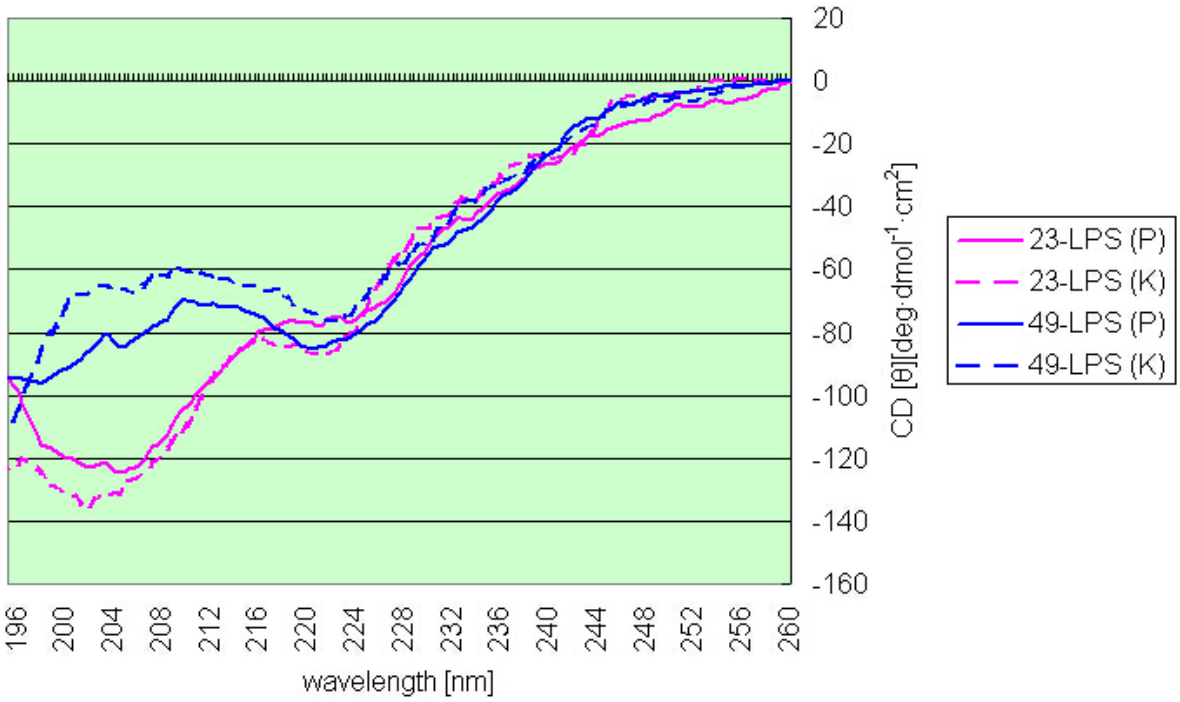

Figure 3.11: CD spectra comparison of peptide **23** and **49** with LPS (P) and (K)

The only structural difference of peptide **49** compared with **23** is the introduction of the nitro- group at the para- position of the phenylalanine benzene ring, and the nitro- group may change the electron distribution within the benzene ring of the phenylalanine and could consequently change the overall physicochemical property of the molecule. However, cautious consideration should be taken that even though the nitro- group is the only structural variance between the two peptides, we can not directly and largely attribute the CD spectra change of peptide **49** to the specific functional group. Due to the complex nature of peptide-LPS interactions, many other factors could also affect the interaction of **49** with LPS and result in a very different spectrum feature.

Background and Discussion of ^{1}H NMR study of peptide-LPS interaction

The CD data shown and discussed above clearly indicates that peptides indeed interact with LPS P and K with various conformation changes. However it should not stop at this point, since the structure of LPS is very complex and there are three components in a complete LPS membrane model: O-antigen, inner core oligosaccharide and the phospholipid-like lipid A. The first two components consist of sugars and more hydrophilic in the buffer environment but the lipid A contains several phospholipids-like acyl long chains which tend to be more hydrophobic. Thus one can expect peptide molecule to interact with any one of the three components, but the question is with which region of LPS the interaction is the most dominant?

^{1}H NMR spectroscopy is a useful tool for structural determination of peptides adopting conformations in membrane model environment and follows the same strategy as NMR structure determination on soluble proteins [33]. A previous study [48] using 1D ^{1}H NMR,

2D ^{1}H TOCSY NMR and diffusion ordered (DOSY) NMR has shown the mechanisms of binding of these AMPs to SDS and DPC micelles are dependent on the physicochemical properties of the AMPs and the micelles. Peptide # 23 was used as an example compound in D_2O sodium acetate buffer and the aromatic resonances was studied in the presence of SDS and DPC micelles. The ^{1}H NMR results showed that the aromatic rings (phenylalanine) of peptide **23** are in very different chemical environment when mixed with SDS and DPC micelles in D_2O sodium acetate buffer and this result is consistent with CD data of peptide **23** with SDS and DPC [29].

In a recent investigation by Hicks R. et al [53], 1D ^{1}H NMR was used to investigate AMP-LPS interactions. There are two major reasons that advanced NMR techniques, such as TOCSY, can not be used to study these AMP-LPS interactions. Firstly at the concentrations of the peptides required to conduct 2D NMR experiments, the peptide-LPS and peptide-phospholipid mixtures precipitated in the buffer thus NMR signals were not detected for the peptide protons. Secondly, the incorporation of three Tic-Oic dipeptide units (these amino acids are secondary amides and therefore lack amide protons) into the sequence of these peptides, coupled with severe overlap of the side chain protons in the region around 2.5- 1.0 ppm, makes the application of 2D experiments very difficult.

CD spectra of peptides with LPS (P) and LPS (K) have shown for each peptide it binds with two different lipopolysaccharide in a similar manner, and the only shared and conserved region of each of the two LPS is the lipid A portion, thus it suggests that the peptides are staying longer and interacting more strongly with the highly conserved lipid A region, rather than highly variable O-antigen and core oligosaccharide regions [53]. Dramatic reduction in

the peak heights of the NMR spectra in the region between 1.5-0.5 ppm was observed when a 1.0 mg/mL sample of LPS (P) in the presence of 0.1 mg of peptide **23**, **29**, **43**, **53** and **56** [53]. Since at this low concentration of peptide NMR signals of peptide protons can not be observed, the said peak heights reduction at 1.5-0.5 ppm should have come from LPS (P) after comparison with the ^{1}H spectrum of LPS (P) alone. This region corresponds to the resonances of $–CH_2-$ acyl side chain protons of lipid A. This observation suggests a strong binding of peptides with the LPS (P) lipid A region, and further inspection of the entire NMR spectrum shows that the other regions of the spectrum remain relatively unchanged on addition of the peptides into LPS (P) solution, which also supports the conclusion that the binding between peptide and LPS (P) occurs in lipid A [53].

A similar peak heights reduction of $–CH_2-$ acyl side chain protons of lipid A was also observed in the spectra of LPS (K) with the addition of peptide, ranging approximately from 1.8 to 0.7 ppm. Again the NMR signals of peptides can not be observed. This suggests that the peptides are interacting with the lipid A region of LPS (K) just like they interact with the lipid A region of LPS (P), a small chemical shift value change may come from tiny structure difference of LPS (K) lipid A from that of LPS (P). Although the peak height reduction of LPS (K) lipid A region is not as dramatic as was observed with the LPS (P), it still supports that peptides interact more strongly with lipid A region of both LPS (P) and LPS (K).

Hicks' conclusion [53] of peptides interacting more strongly with lipid A acyl side chain can be supported by the results of Brandenburg, K et al. [49]. In this study a synthetic triacyl glucosamine monosaccharide lipid A part structures corresponding to the non-reducing moiety of bacterial lipid A was analyzed biophysically. Fourier-transform infrared

spectroscopy (FTIR) was used to characterize the gel-to-liquid crystalline phase transition of lipid A. The FTIR shows that the temperature dependence of the peak position of the symmetric stretching vibration $\nu_s(CH_2)$ indicates a gel-to-liquid crystalline phase transition of the acyl chains. In another peptide-LPS interaction study by the same author [50], the peptide binds to LPS with a high affinity and induces a change in the lipid A region and suggested a hydrophobic interaction between the peptide and the hydrocarbon chain region of lipid A.

Lastly, the only uncertain aspect of the NMR study is the reason behind the peak heights reduction of lipid A $-CH_2-$ acyl side chain. Hicks R. et al [53] proposed that the phenomenon is the increase of the T_1 relaxation rates of lipid A acyl chain protons. C. Le Guerneve et al [51] showed the incorporation of cholesterol into DMPC (dimyristoylphosphatidylcholine) has an effect on the high frequency vibrations that contribute to T_1 relaxation inducing longer T_1 relaxation. They further explained that cholesterol restricts the high frequency motions of the acyl chains thus increasing the molecular order of these regions compared to the pure lipid bilayer..

Results of 1D ^{1}H NMR

AMP #	Peak area normalized to LPS (P) alone
23	38%
29	38%
43	36%
53	29%
56	39%

Table 3.7: Changes in peak area of the proton resonances in the region of 1.5-0.5 ppm of the spectra of LPS (P) as a function of the addition of a specific peptide [53]

AMP #	Peak area normalized to LPS (K) alone
23	81%
29	80%
43	93%
53	89%
56	81%

Table 3.8: Changes in peak area of the proton resonances in the region of 1.8-0.7 ppm of the spectra of LPS (K) as a function of the addition of a specific peptide [53]

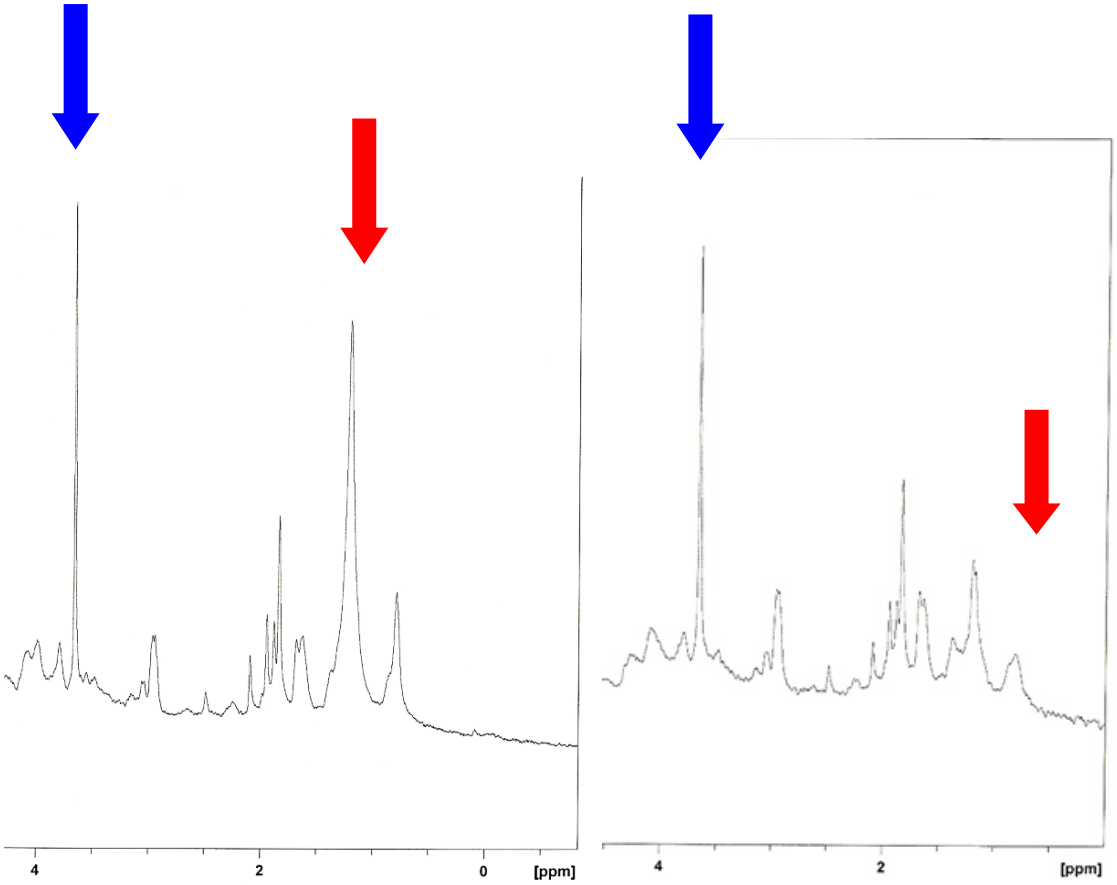

Figure 3.12: (Left) 1D ^{1}H NMR of LPS (P) ONLY in 150 mM perdeuterated sodium acetate buffer at a pH of 5.64 in D_2O; (Right) 1D ^{1}H NMR of LPS (P) plus peptide **23** in the same buffer. All LPS and peptide concentrations in NMR study keep consistent. Blue arrow shows peak of carbohydrate (sugar moiety) protons in LPS (P) and red arrow shows peak of acyl side chain –CH_2- protons in lipid A. All spectra have been processed into the same scale [53].

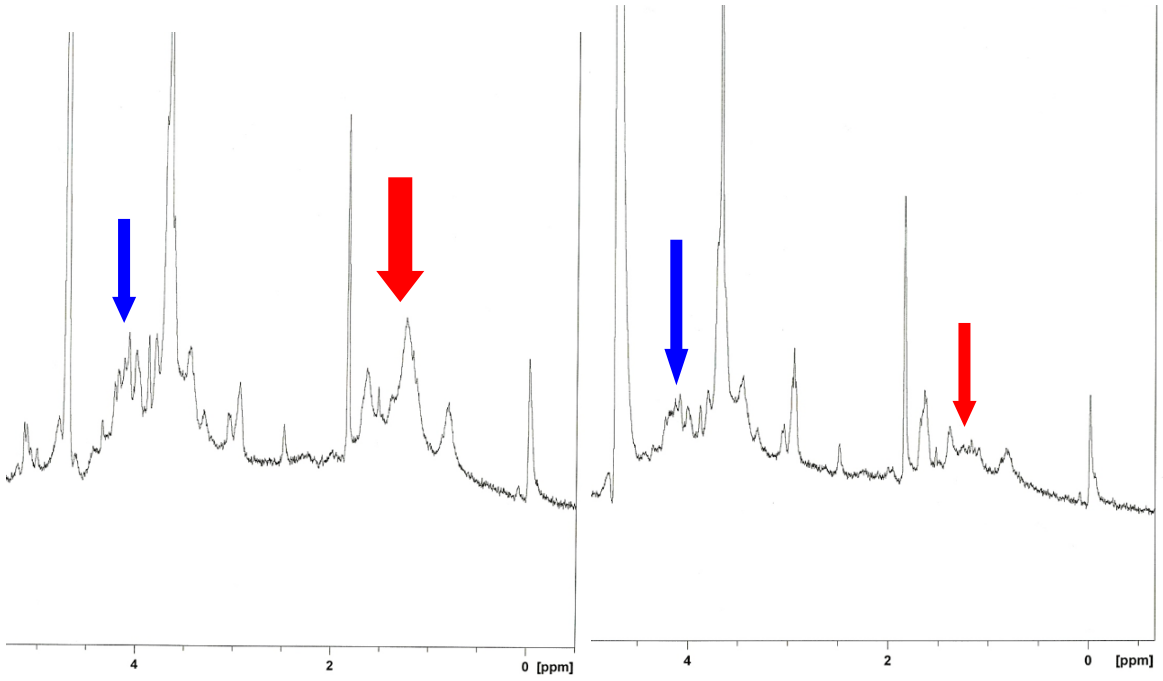

Figure 3.13: (Left) 1D ^{1}H NMR of LPS (K) ONLY in 150 mM perdeuterated sodium acetate buffer at a pH of 5.64 in D_2O; (Right) 1D ^{1}H NMR of LPS (K) plus peptide **23** in the same buffer. All LPS and peptide concentrations in NMR study keep consistent. Blue arrow shows peak of carbohydrate (sugar moiety) protons in LPS (K) and red arrow shows peak of acyl side chain –CH_2- protons in lipid A. All spectra have been processed into the same scale [53].

3.1.2 Liposome System Two and Three: Inner Membrane Phospholipid Models of Gram-negative *Bacteria Pseudomonas aeruginosa* and *Klebsiella pnemoniae* and complete Outer Membrane of the two strains-A comparative study

The inner membrane and the phospholipids components of outer membrane of Gram-negative bacteria mostly consist of phospholipids. The natural *Pseudomonas aeruginosa* lipid consists of 21% POPG, 60% POPE and 11% caridiolipin [52]. For *Klebsiella*

pnemoniae it consists of 5% POPG, 82% POPE and 6% caridiolipin [52]. POPC and POPE are zwitterionic and POPG, caridiolipin are all anionic. The total percent of anionic lipids for *Pseudomonas aeruginosa* and *Klebsiella pneumoniae* are 32% and 11%, respectively [5]. In this project, **59% POPC/21% POPG/20% POPE (mix P)** is used to approximate the lipid composition (molar ratio) of *Pseudomonas aeruginosa* and **75% POPC/5% POPG/20% POPE (mix K)** for *Klebsiella pneumoniae.* The highest percentage of POPE can reach is 20% out of total lipid because we also tested that when the percentage goes beyond 20% dramatic precipitates can form when mix the lipid solution with peptide stock solution.

In this section, CD spectra of peptides in the presence of inner membrane composition (mix P and K) will be compared with CD spectra of peptides in the presence of complete outer membrane (LPS-mix P and K), in the presence of LPS only (P and K), as well as the CD spectra of peptide alone in the phosphate buffer.

Results: CD spectra of peptide alone, peptide-mix (P or K) and peptide-LPS-mix (P or K). Buffer line has been subtracted from peptide alone spectra and any lipid composition (mix or LPS-mix complex) has been subtracted from peptide-lipid spectra so all show the **CD spectra of peptides** in different chemical environments.

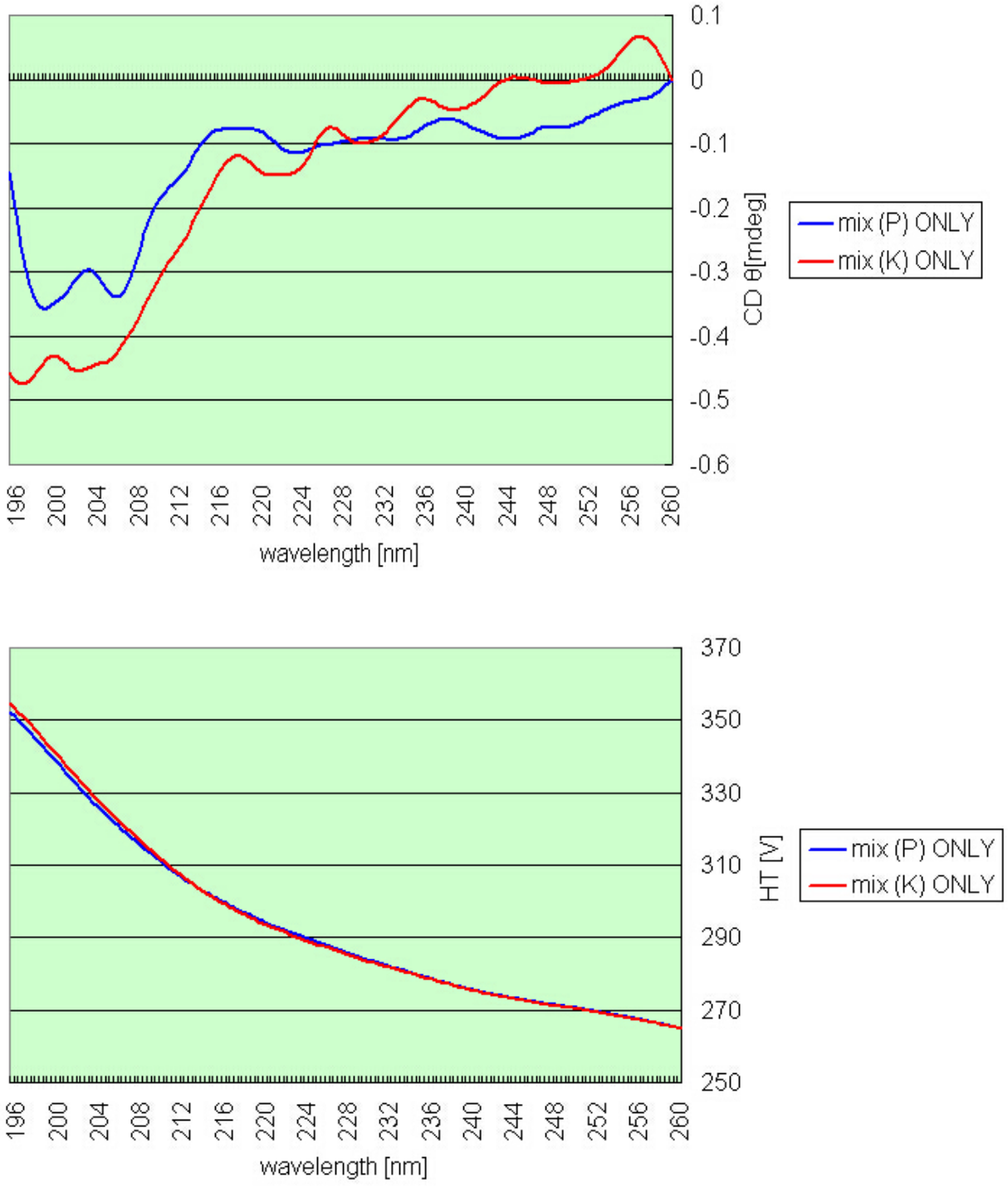

Figure 3.14: (Top) CD spectra of phospholipid composition mix (P) and mix (K); (bottom) HT value curve of mix (P) and mix (K) in buffer. Millidegree is used as the CD data unit.

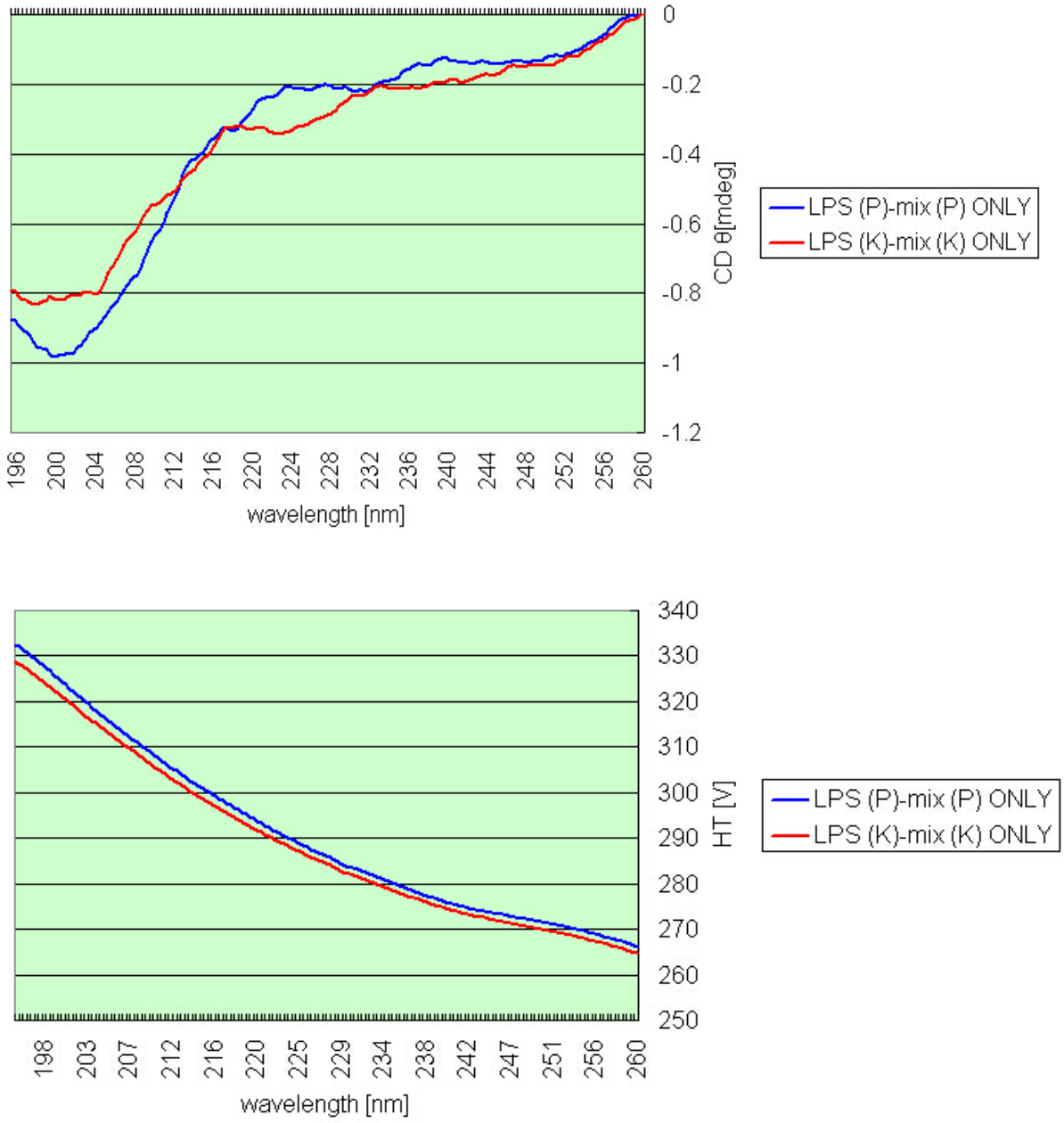

Figure 3.15: (Top) CD spectra of LPS-mix (P or K) complex alone in the phosphate buffer; (bottom) HT value curve of LPS-mix (P) and LPS (K)-mix (K) in buffer. Millidegree is used as the CD data unit. Due to the incorporation of LPS, CD negative band at ~ 200 nm is still observable. Thus subtraction of the lipid line from peptide-lipid line is always necessary, even though CD spectra of lipid models are very weak.

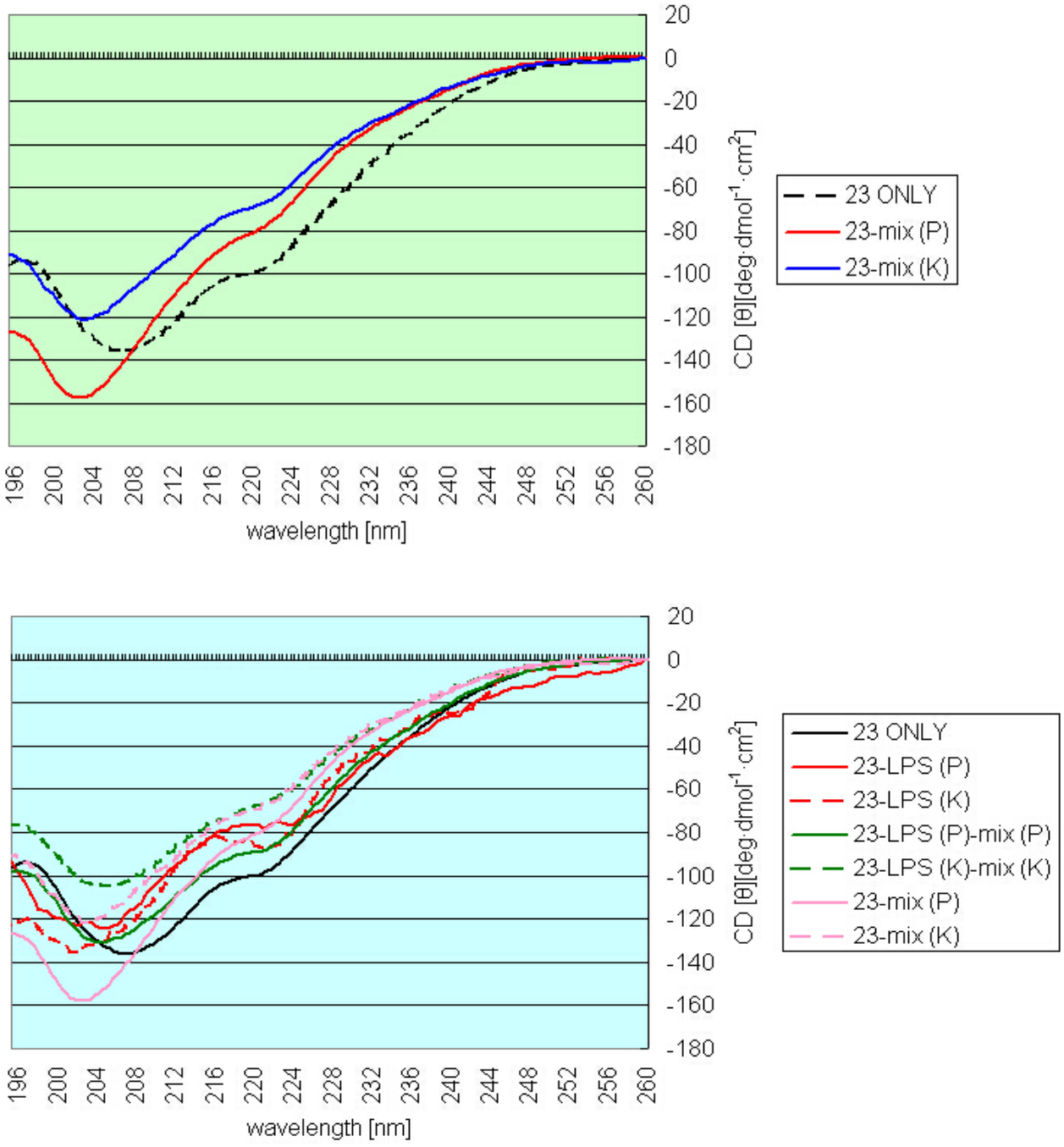

Figure 3.16: (Top) CD spectra of peptide **23** alone (dashed line, **black**), peptide **23** with inner membrane composition from *Pseudomonas aeruginosa* (P) (solid line, **red**) and *Klebsiella pneumoniae* (K) (solid line **blue**) in phosphate buffer converted into molar ellipticity [θ].

(Bottom) CD spectra comparison of peptide **23** with all three lipid model systems: peptide **23** alone in buffer (solid line, **black**), peptide **23** with LPS (P) and (K) (solid & dashed line, **red**), peptide **23** with LPS-mix (solid & dashed line, **green**) and with mix (solid & dashed, **pink**).

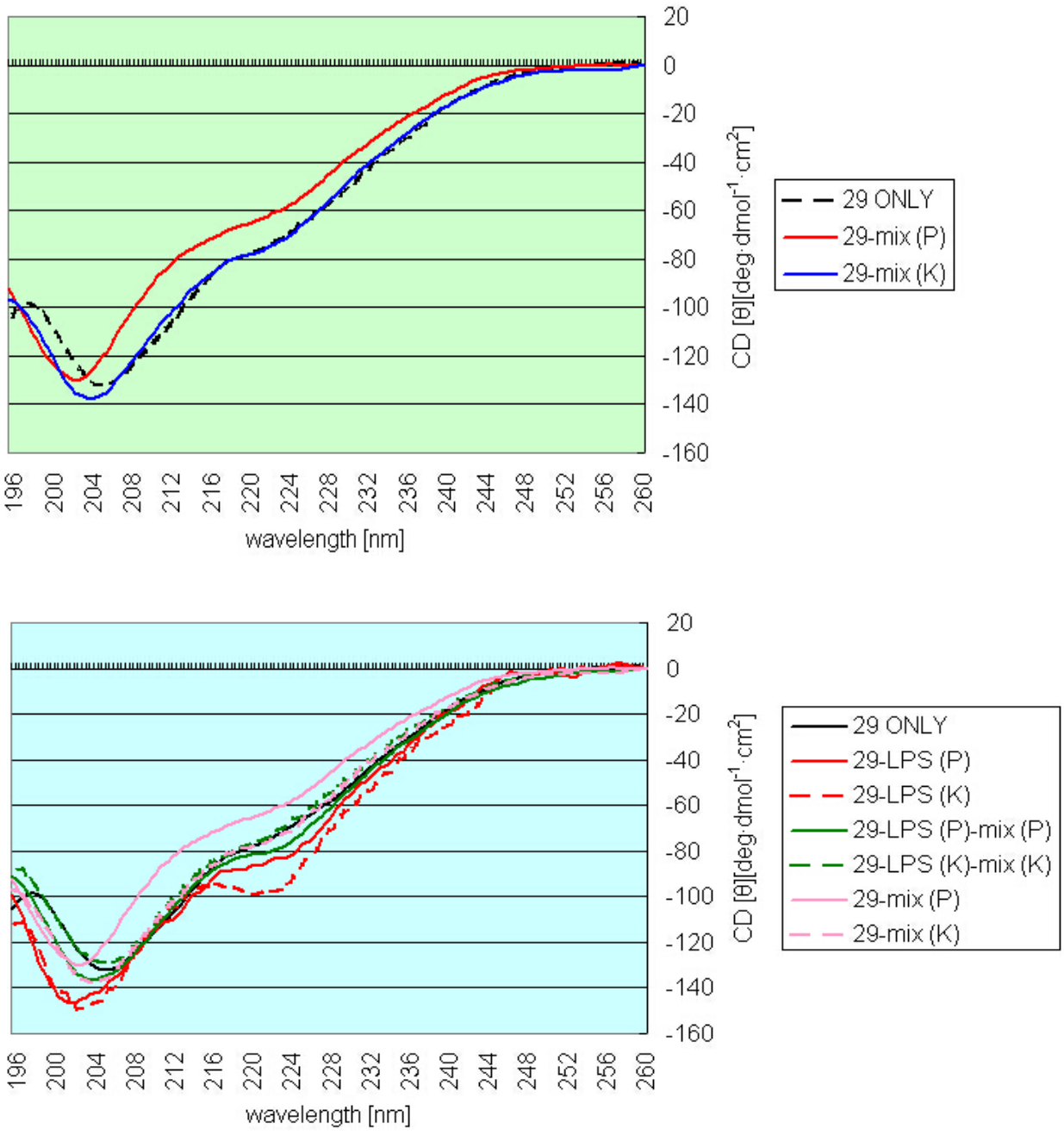

Figure 3.17:(Top) CD spectra of peptide **29** alone (dashed line, **black**), peptide **29** with inner membrane composition from *Pseudomonas aeruginosa* (P) (solid line, **red**) and *Klebsiella pneumoniae* (K) (solid line **blue**) in phosphate buffer converted into molar ellipticity [θ].

(Bottom) CD spectra comparison of peptide **29** with all three lipid model systems: peptide **29** alone in buffer (solid line, **black**), peptide **29** with LPS (P) and (K) (solid & dashed line, **red**), peptide **29** with LPS-mix (solid & dashed line, **green**) and with mix (solid & dashed, **pink**).

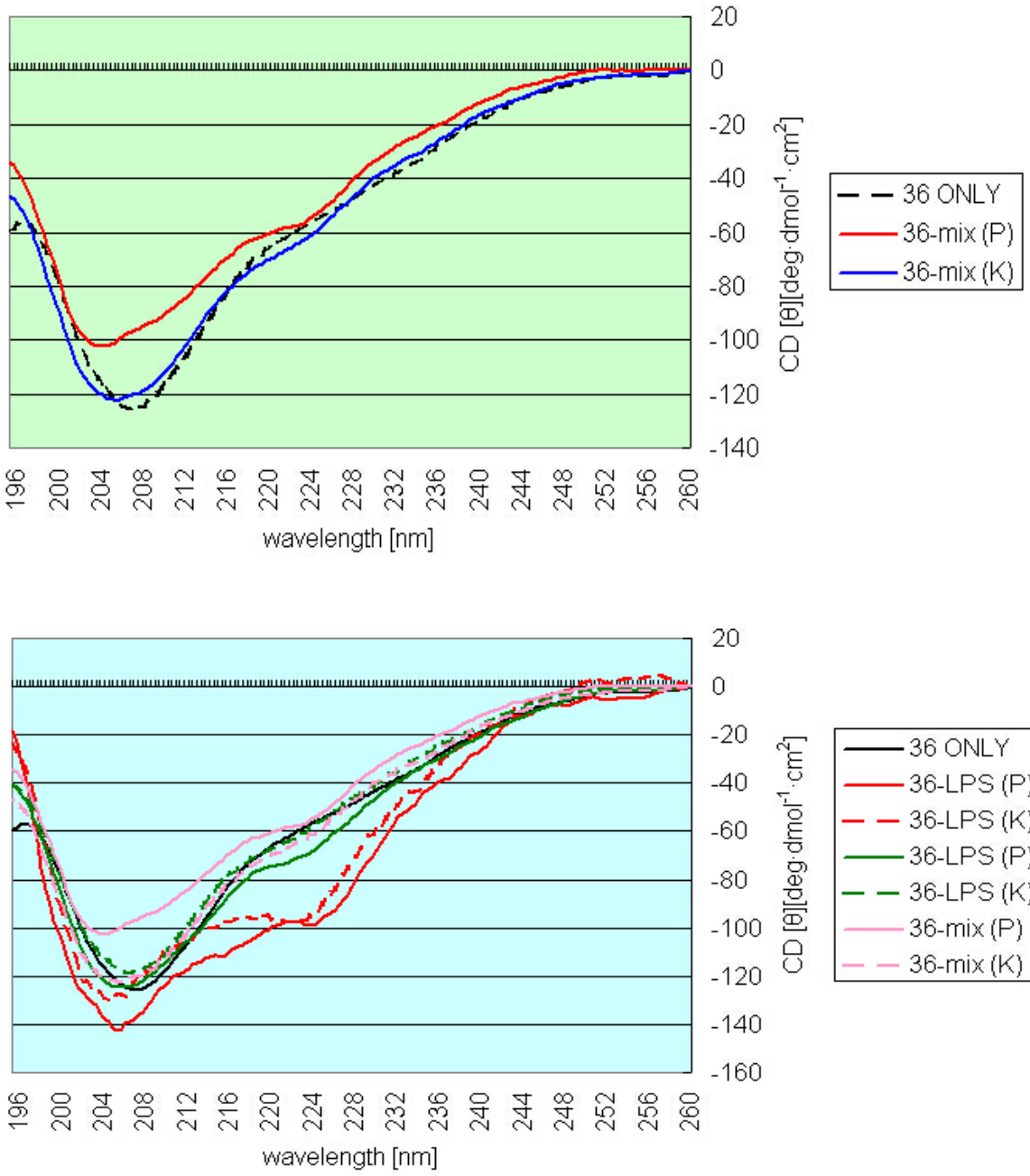

Figure 3.18 (Top) CD spectra of peptide **36** alone (dashed line, **black**), peptide **36** with inner membrane composition from *Pseudomonas aeruginosa* (P) (solid line, **red**) and *Klebsiella pneumoniae* (K) (solid line **blue**) in phosphate buffer converted into molar ellipticity [θ].

(Bottom) CD spectra comparison of peptide **36** with all three lipid model systems: peptide **36** alone in buffer (solid line, **black**), peptide **36** with LPS (P) and (K) (solid & dashed line, **red**), peptide **36** with LPS-mix (solid & dashed line, **green**) and with mix (solid & dashed, **pink**).

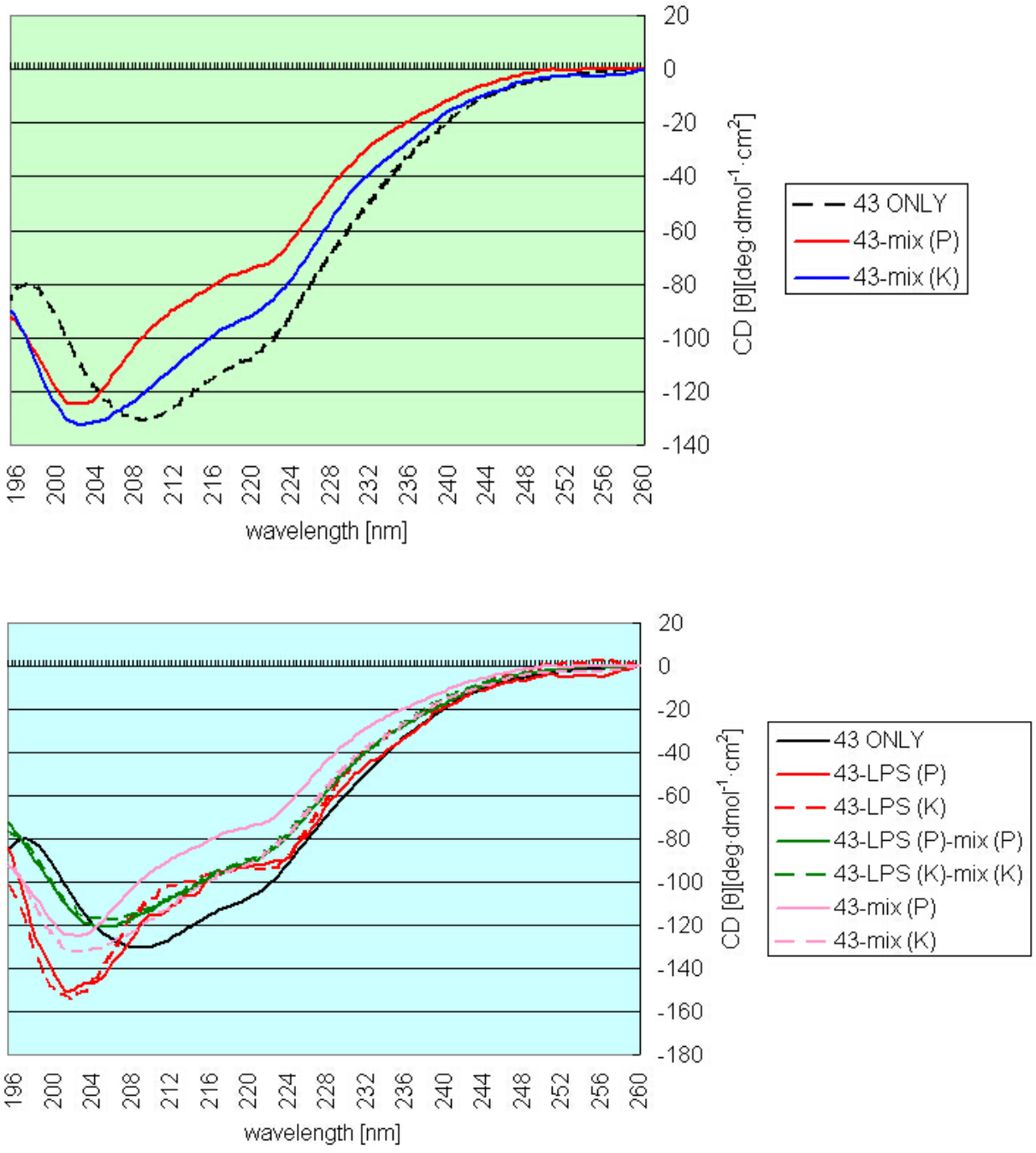

Figure 3.19: (Top) CD spectra of peptide **43** alone (dashed line, **black**), peptide **43** with inner membrane composition from *Pseudomonas aeruginosa* (P) (solid line, **red**) and

Klebsiella pneumoniae (K) (solid line **blue**) in phosphate buffer converted into molar ellipticity [θ].

(Bottom) CD spectra comparison of peptide **43** with all three lipid model systems: peptide 43 alone in buffer (solid line, **black**), peptide **43** with LPS (P) and (K) (solid & dashed line, **red**), peptide **43** with LPS-mix (solid & dashed line, **green**) and with mix (solid & dashed, **pink**).

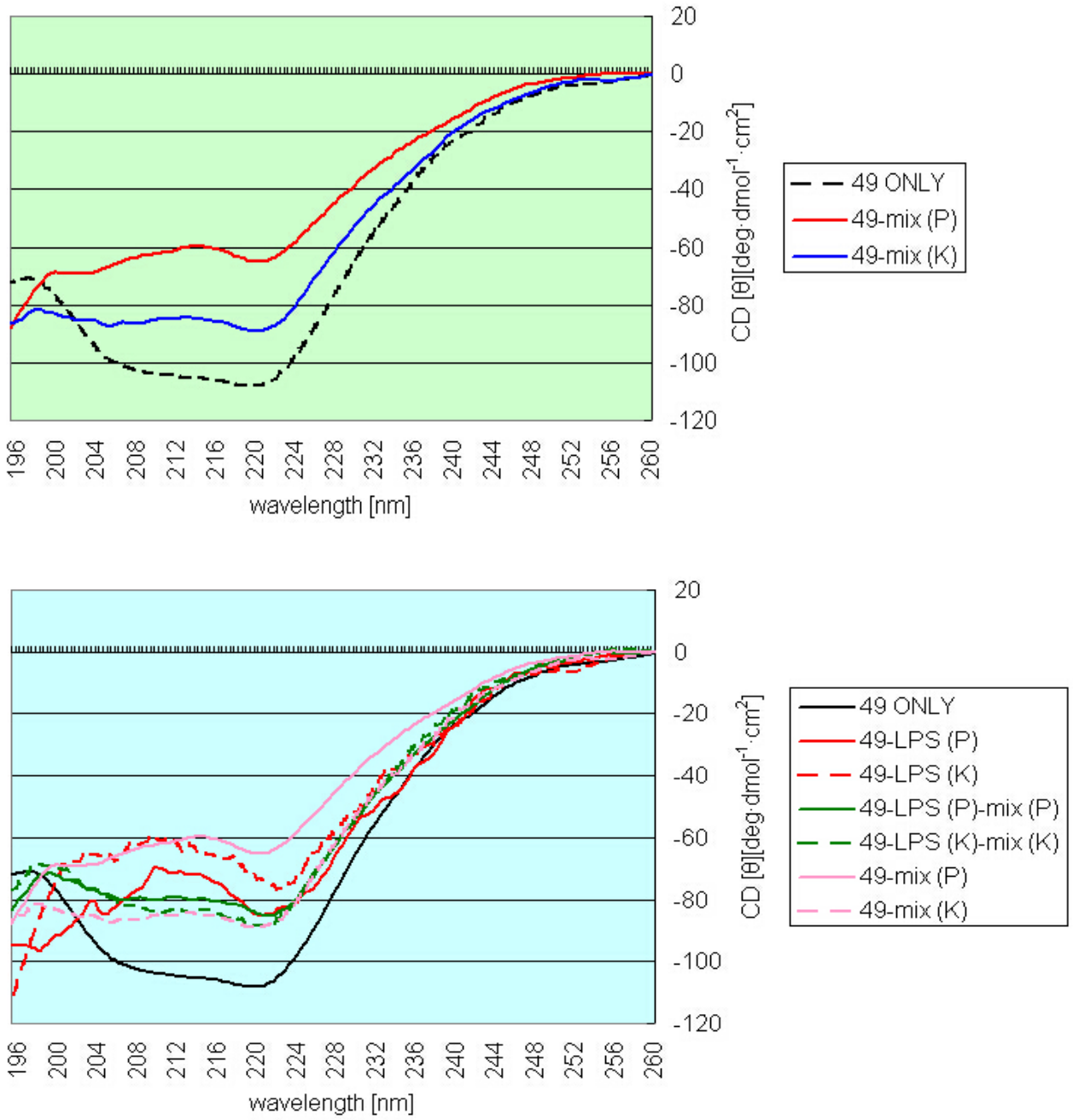

Figure 3.20: (Top) CD spectra of peptide **49** alone (dashed line, **black**), with inner

membrane composition from *Pseudomonas aeruginosa* (P) (solid line, **red**) and *Klebsiella pneumoniae* (K) (solid line **blue**) in phosphate buffer converted into molar ellipticity [θ].(Bottom) CD spectra comparison of peptide **49** with all three lipid model systems: peptide alone in buffer (solid line, **black**), with LPS (P) and (K) (solid & dashed line, **red**), with LPS-mix (solid & dashed line, **green**) and with mix (solid & dashed, **pink**).

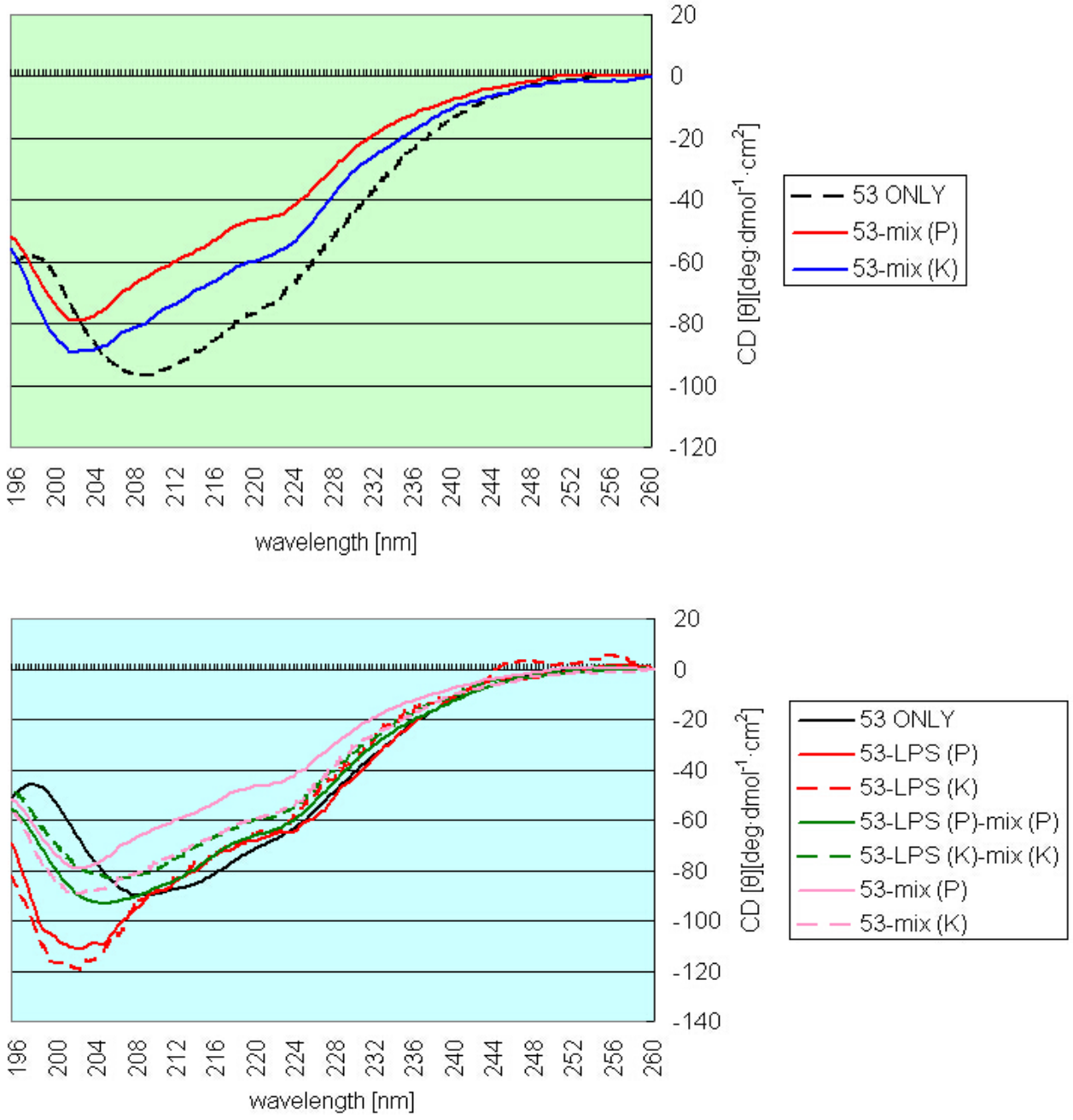

Figure 3.21: (Top) CD spectra of peptide **53** alone (dashed line, **black**), with inner

membrane composition from *Pseudomonas aeruginosa* (P) (solid line, **red**) and *Klebsiella pneumoniae* (K) (solid line **blue**) in phosphate buffer converted into molar ellipticity [θ].(Bottom) CD spectra comparison of peptide **53** with all three lipid model systems: peptide alone in buffer (solid line, **black**), with LPS (P) and (K) (solid & dashed line, **red**), with LPS-mix (solid & dashed line, **green**) and with mix (solid & dashed, **pink**).

Discussion

For the individual peptide, its three sets of CD spectra of interacting with three different membrane model compositions (LPS only, mixed phospholipid and LPS-phospholipid complex) are compared in one figure. Firstly when red lines (with LPS only) and green lines (with LPS-mix complex) are compared, it is apparent that each peptide interacts with the two models differently, which reveals an important information that LPS and LPS-mix complex have become two different chemical environments. Additionally, the spectra of peptide with LPS-mix complex (green) can not be obtained from simple spectra addition of the peptide with LPS only (red) and with mix only (pink). Thus it suggests that LPS and phospholipid have been incorporated together to make a LPS-mix SUV. It can be inferred, but can not be proved, under current experimental circumstances of this project, that the outer leaflet of the SUVs will contain a higher percentage of LPS as compared to the inner leaflet will contain almost exclusively phospholipids, there is no direct solid evidence that LPS is not incorporated in inner leaflet of membrane either. However, even if this is not the case and the LPS is randomly distributed over both the inner and outer leaflets, at least it suggests that LPS and phospholipids are incorporated to make a new liposome which is not the simple

physical mixture of the two. It still can be regarded as a combined effect of LPS and phospholipids on peptide binding. Thus this discussion is qualitative analysis of CD spectra.

Secondly, for each peptide, the shapes of spectra of peptide with phospholipid model, mix (P) (red) and mix (K) (blue), are similar in shape but are both different with spectrum of peptide alone in buffer, supporting that peptide changes conformation when it interacts with an inner membrane model of bacteria. For mix (P), there is a good positive correlation between the extent of the side chain positive charge delocalization and the intensity (23(Lys) >43(Orn) >53(Dab) >56(Arg) >46(Dpr))of the CD spectra. For these peptides the first negative peak values in the presence of only phospholipid are blue-shifted compared to the LPS-containing SUVs by about 2-4 nm, indicating a small change in the conformations upon binding with mix (P).

When CD spectra of the same peptides interacting with mix (K) and LPS (K)-mix (K) are compared, useful information can be extracted about the conformational change of peptides traveling from the outer membrane to the inner membrane. For example, CD spectra of peptide **43** with mix (K) (pink dashed line in **43** comparison set) and LPS (K)-mix (K) (green dashed line in # 43 comparison set) are different both in intensity (the former is less intense than the latter) and shape, indicating peptide **43** changes conformation while migrating from the outer membrane to the inner membrane, and the interaction with the outer membrane model LPS (K)-mix (K) is stronger. A similar trend is also observed in peptide **53** interacting with complete outer membrane of LPS-mix (P and K) and with inner membrane of mix (P and K).

The comparison trend (red lines in bottom spectra) of each peptide interacting with LPS (P)-mix (P) and LPS (K)-mix (K) is complicated. For some peptides, such as **23** and **53**, the molecular flexibility in the presence of LPS (K)-mix (K) is greater than with LPS (P)-mix (P) and for **43**, flexibility and conformation with both models are almost the same. Such scenario is probably brought by the introduction of phospholipids into LPS. More specifically, it is partially due to surface charge difference between two phospholipid models. Mix (P) has 21% of the anionic lipid POPG while mix (K) has only 5% POPG. The more essential reason behind the complexity, of course, lies in the physicochemical properties of peptide SPACER #2.

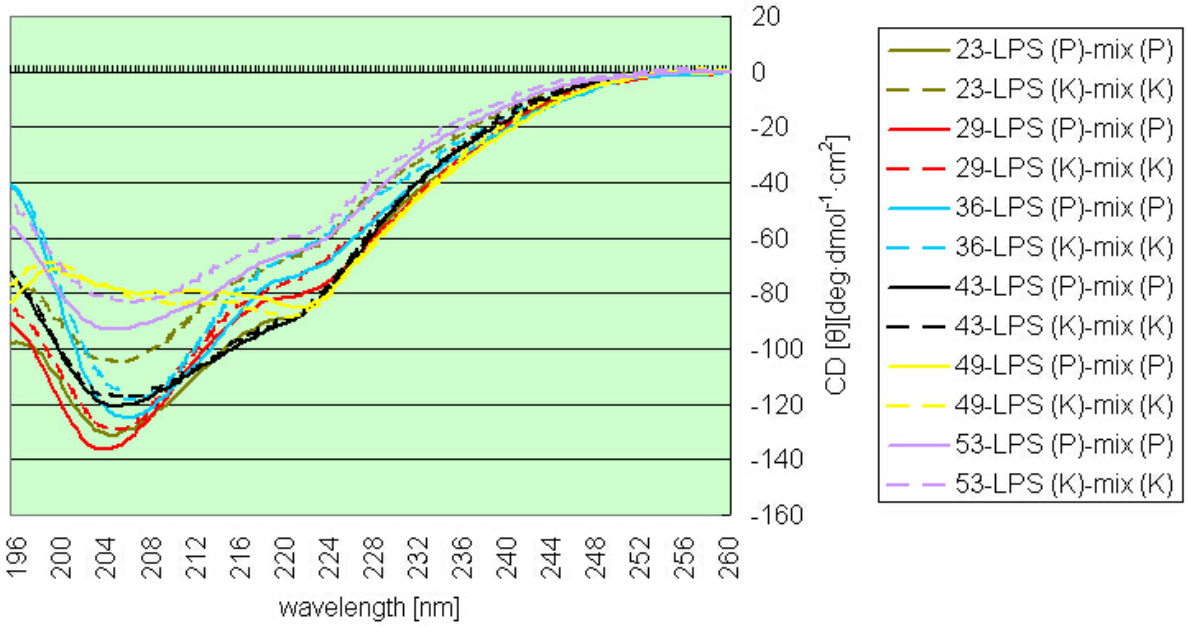

Figure 3.22: CD spectral comparison of all peptide interacting with complete outer membrane models of *Pseudomonas aeruginosa* (solid lines) and *Klebsiella pneumoniae* (dashed lines).

It is immediately obvious that for peptide **43 (black)** the interaction with both models are almost the same. The hydrophobicity of the Orn residues of **43** is the highest (-9.0) of the

SPACER#2 residues, while the charge delocalization is the second lowest. Contributions from hydrophobicity and the extent of the positive charge delocalization of SPACER#2 side chain and the two factors balance out to make the CD spectra of **43** with both models almost the same. Such a phenomenon is also observed in **49** (yellow).

It can be concluded, by studying CD spectra together with the consideration of the physicochemical properties of the SPACER, that the binding of peptides with the complete outer membrane models of *Pseudomonas aeruginosa* and *Klebsiella pneumoniae* does not simply depend on electrostatic interactions. The binding process is a complex balance between electrostatic and hydrophobic effects which makes each peptide interact with the two models differently. However, a precise correlation between peptide physicochemical properties and conformational change is very challenging under the current experimental technique limitations.

3.2 Proposed Mechanism of AMPs Interacting with Gram-Negative Bacteria Cell Wall and Antimicrobial Activities of AMPs towards *Pseudomonas aeruginosa* and *Klebsiella pneumoniae*

After collecting all conformational change information from peptides interacting with the three membrane models, we proposed a possible mechanism of action towards Gram-negative bacteria cell membrane in a recent publication [53]. There are eight consecutive steps for a peptide molecule to travel through and bind with a cell membrane. Step A shows the initial binding of the peptide from the aqueous extracellular environment to the O-antigen, the outer component of LPS. Step B shows the transport of the AMP from the

O-antigen, through the core oligosaccharide, to the surface of Lipid A. This is also the time when the peptide interacts with the lipid A acyl side chains. Step C represents the transport of the peptide through lipid A of the LPS to the phospholipid component of the inner leaflet. In Step D, the peptide goes across the phospholipid layer of the inner leaflet. Step E represents the conformational changes that may occur in the periplasmic space between the outer and inner membranes. Step F represents the binding and conformational changes associated with a single peptide molecule interacting with the surface of the phospholipids of the inner membrane outer leaflet. Step G represents the oligomerization of peptide molecules interacting with the surface of the phospholipids of the outer leaflet of the inner membrane prior to insertion into the membrane. Step H [29] represents the transition from the surface bound state to the membrane inserted state which results in disruption of the inner membrane.

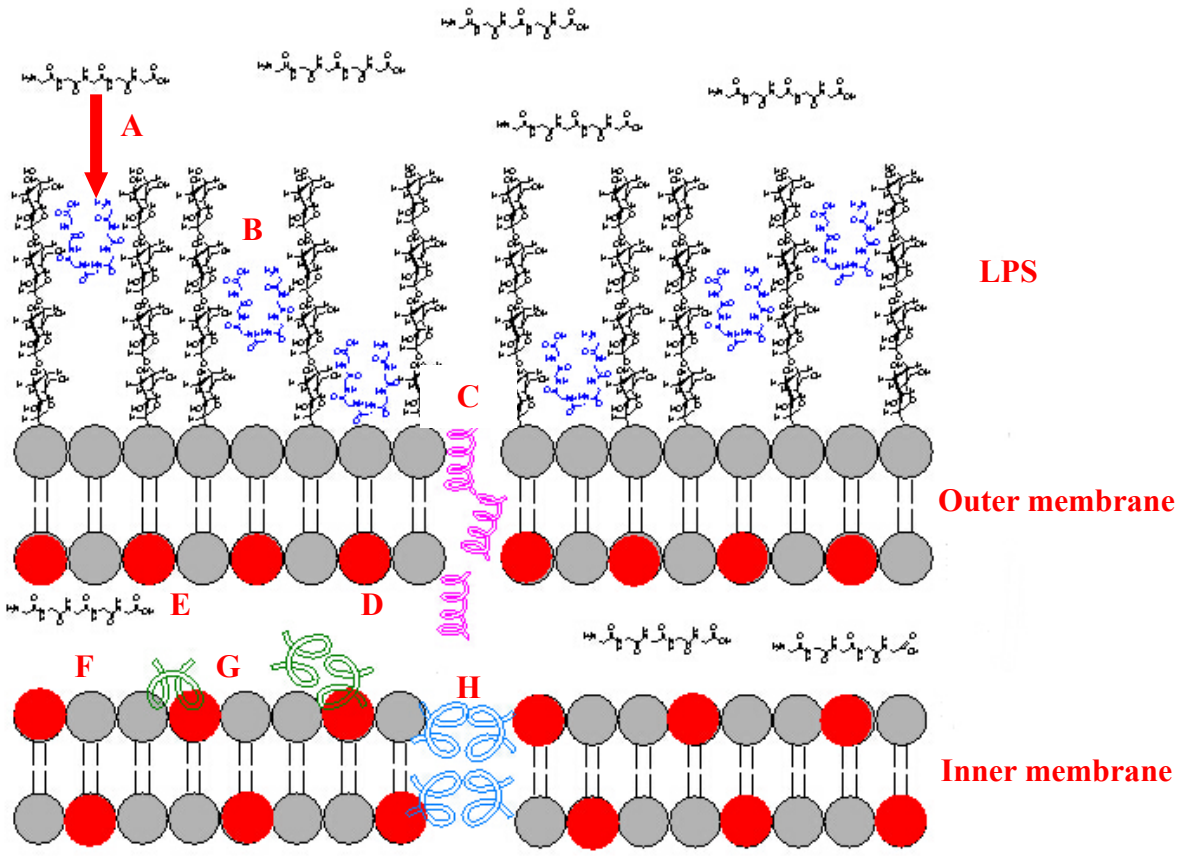

Figure 3.23: A cartoon representation showing the proposed binding and transport mechanism of a peptide with the outer and inner membranes of Gram-negative bacteria

CD spectroscopy is a powerful tool for studying the conformational changes of optically active compounds when they bind to other ligand molecules. However this biophysical technique can not give detailed structural information like NMR. Though it is attempting to try correlating the peptide binding behavior represented in CD spectra with the antimicrobial activity, the action mechanism of peptides towards pathogenic microbes is very sophisticated. One single factor, side chain positive charge density for instance, is far from sufficient to fully account for specific peptide activity.

	Pseudomonas aeruginosa PAO1		*Klebsiella pneumoniae* BAMC 07-18	
Peptide #	MIC (μg/mL)	MBC (μg/mL)	MIC (μg/mL)	MBC (μg/mL)
23	100	100	100	100
29	＞100	＞100	100	100
36	＞100	＞100	＞100	＞100
43	50	50	50	50
46	25	50	12.5	25
49	50	100	50	50
53	12.5	12.5	12.5	12.5
56	100	＞100	50	100

Table 3.9: In vitro susceptibility of antimicrobial peptides toward *Pseudomonas aeruginosa and Klebsiella pneumoniae* [5]

From the MIC and MBC data of the eight investigated peptides, the peptides probably interact with LPS (P) and (K) similarly because for each peptide relevant concentrations toward the two strains are very close. This has been supported by the similar intensity and shape of CD spectra of peptides binding to LPS (P) and (K). Secondly, among the eight peptides, peptides **46** and **53** are relatively more active than the others. Previous CD studies in section 3.1.2 have shown that the two peptides bind with LPS-mix more strongly than binding with the inner membrane model mix only, and within the process of peptide binding with the outer membrane, the interaction between peptide and lipid A region is more crucial for membrane disruption [51]. Thus, lower MIC and MBC concentrations of peptide **46** and **53** can impart better perturbation on the lipid A region than the other less active peptides in the list.

Final Conclusion

(1) The interactions between the peptides and membranes are defined by the complementary effects of several essential physicochemical properties of the peptides. Delocalization of positive charge density of the basic amino side chains which is controlled by SPACER # 2; molecular flexibility of the peptide backbone and overall hydrophobicity which is controlled by SPACER # 1 and # 2 together. The relative contribution of each of these key physicochemical properties depends on the composition of the model system investigated (i.e. the percentage of anionic lipids).

(2) The peptides show a higher partition coefficient for the lipid A region than for the O-antigen or core oligosaccharide regions of the LPS, which is supported by 1 D ^{1}H NMR.

(3) Incorporation of phospholipids into the LPS-containing phospholipid SUVs results in pronounced changes in the conformation of the bound peptides.

REFERENCES

1. Davies, J.; Davies D. *Microbiol Mol Biol Rev*. **2010**; 74 (3), 417–433.
2. Swann, J. *Brit J Hist Sci*, **1983**; 16 (2), 154-190.
3. Chain, E.; Abraham, E. P. *Nature*. **1940**; 146, 837-837.
4. Dalton, T.; Cegielski, P. *Lancet*, **2012**, 380, 1406–1417.
5. Hicks, R. P.; Leung, K. P. *Bioorg. Med. Chem.* **2013**, 21, 205–214.
6. *Brock Biology of Microorganisms,* 2010*,* Benjamin Cummings, 13th edition.
7. Huycke, M. M.; Sahm, D. F.; Gilmore, M. S. *Emerging Infect. Dis.* **1998**, 4 (2), 239-249.
8. Mascini, E. M.; Troelstra, A. *Clin Infect Dis*. **2006**, 42, 739–746.
9. *NIH News*, **1999**, May 27.
10. Chambers, H. F. *Emerging Infect. Dis.* **2001**, 7 (2), 178-182.
11. Enright, M. C.; Robinson, D. A.; Randle, G.; Feil, E. J.; Grundmann, H.; Spratt, B. G. *Proc. Natl. Acad. Sci.* U.S.A. 2002, 99 (11), 7687–7692.
12. Hancock, R. E. W. *Ann. Rev. Microbiol*. **1984**, 38, 237-64.
13. Raetz, C. R. H.; Chris, W. *Annu. Rev. Biochem*. **2002**, 71, 635-700.
14. Bhunia, Anirban.; Mohanram, H.; Domadia, P. N.; Torres, J.; Bhattacharjya, S. *J Biol Chem.* **2009**, 284 (33), 21991–22004.
15. Rice, L. B. *J. Infect. Dis.* **2008**, 197, 1079–1081

16. Drummond, K. “Pentagon to Troop-Killing Superbugs: Resistance Is Futile”, May 24, **2010**

17. Balcht, A.; Smith, R. *Pseudomonas aeruginosa: Infections and Treatment.* Informa Health Care, **1994**.

18. Izadpanah, Arash.; Gallo, R. L. *J. Am. Acad. Dermatol,* **2005**, 52, 381-390.

19. Hancock, R. E. W.; Lehrer, R. *Trends Biotechnol*. **1998**, 16 (2), 82-88.

20. Howden, B. P.; Davies, J, K.; Johnson, P. D. R.; Stinear, T. P.; Grayson, M. L. *Clin. Microbiol. Rev.* **2010**, 23 (1), 99-139.

21. Chang, S-J, Sievert, M. D.; Hageman, J. C.; Boulton, M. L.; *N. Engl. J. Med.* **2003**, 348, 1342-1347.

22. Hancock, R. E. W. *The Lancet*, **1997**, 349 (9049), 418-422.

23. Ostberg, N.; Kaznessis, Y. *Peptide*. **2005**, 26 (2), 197-206.

24. Brogden, K. A. *Nature Rev. Microbiol*. **2005**, 3, 238-250.

25. Zasloff, M. *Nature*. **2002**, 415 (6870), 389 – 395.

26. Hicks, R. P.; Mones, E.; Kim, H.; Koser, W. B.; Nichols, A. D.; Bhattacharjee, K. A. *Biopolymers*. **2003**, 68 (4), 459 – 470.

27. Hicks, R. P.; Bhonsle, B. J.; Venugopal, D.; Huddler, P. D.; Magill, J. A.; *J. Med. Chem*. **2007**, 50 (26), 6545–6553.

28. Hicks, R. P.; Bhonsle, B. J.; Venugopal, D.; Koser, W. B.; Magill, J. A. *J. Med. Chem*. **2007**, 50, 3026-3036.

29. Epand, R. M.; Vogel, H. J. *Biochimica et Biophysica Acta*. **1999**, 1462, 11-28.

30. Matsuzaki, K. *Biochimica et Biophysica Acta*. **1998** (1376), 391-400.

31. Bhunia, A.; Domadia, N. P.; Torres, J.; Hallock, J. K.; Ramamoorthy, A.; Bhattacharjya, S. *J. Biol. Chem.* **2010** (285), 3883-3895.

32. Domadia, P. N.; Bhunia, A.; Ramamoorthy, A.; Bhattacharjya, S. *J. Am.Chem. Soc.* **2010** (132), 18417-18428.

33. Wang, X.; Quinn, P. J. *Prog Lipid Res*. **2010** (49), 97–107.

34. Raetz, C. R. H. J Lipid Res. **2009** (50), S103-S108.

35. Grant, G. A. *Synthetic Peptides, A user's guide*. New York, NY: Oxford University Press, **2002**.

36. Benoiton, N. L. *Chemistry of Peptide Synthesis*. Boca-Raton, Fl: Taylor and Francis (CRC Press), **2006**.

37. Wieprecht, T.; Apostolov, O.; Seelig, *J. Biophysical Chem*.**2000** (85), 187-198.

38. Ding, L.; Yang, L.; Weiss, T. M.; Warning, A. J.; Lehrer, R. I.; Huang, H. W. *Biochemistry*. **2003** (42), 12251-12259.

39. Matsuzaki, K.; Sugishita, K.-I.; Miyajima, K. *FEBS Letts*, **1999** (449), 221-224.

40. Russell, A. L.; Kennedy, A. M.; Spuches, A.; Venugopal, D.; Bhonsle, J. B.; Hicks, R. P.. Chem. Phys. Lipids. **2010** (163), 488-497.

41. Hershberger, C.; Binkley, S. B. *J. Biol. Chem.* **1968** (243), 1578-1584.

42. Tzeng, Y-L.; Datta, A.; Kolli, V. K.; Carlson, W. R.; Stephens, S. D. J. Bacteriol. **2002**, 184(9), 2379-2388.

43. Ryder, M. P. *Dissertation for the degree of Doctor of Philosophy*: *Binding of Bacterial Lipopolysaccharide by the Cationic Amphiphilic Peptide WLBU2 at Interfaces.* **2014**.

44. Petsch, D.; Anspach, F. B. *J. Biotech.* **2000** (76), 97–119.

45. Kuehn, M. J.; Kesty, N. C. *Genes Dev*. **2005** (19), 2645-2655.

46. Pier, G. B. *International Journal of Medical Microbiology*. **2007** (297), 277–295.

47. Vinogradov, E.; Frirdich, E.; MacLean, L. L.; Perry, B. M.; Petersen, O. B.; Duus, Ø. J.; Whitfield, C. *J. Biol. Chem.* **2002** (277), 25070-25081.

48. Clark, T. D.; Bartolotti, L.; Hicks, R. P. *Biopolymers.* **2013**, 99 (8). 548-561.

49. Brandenburg, K.; Matsuura, M.; Heine, H.; Muller, M.; Kiso, M.; Ishida, H.; Koch, J. M. H.; Seydel, U. *Biophys. J.* **2002** (83), 322–333.

50. Andra, J.; Koch, J. M. H.; Bartels, R.; Brandenburg, K. *Antimicrob. Agents Chemother*. **2004**, 48 (5), 1593–1599.

51. Guerneve, C. L.; Auger, M. *Biophys. J.* **1995**, 68, 1952-1959.

52. Epand, R. M.; Epand, R. F. *J. Pept. Sci*. **2011**, 17, 298–305.

53. Hicks, R. P.; Chai, H-B.; Allen, W. *Bioorg. Med. Chem*. 2014, *In Press.*

54. Brandenburg K. *Eur. J. Biochem*. **2002**, 269, 5972–5981

55. Johnson, W. C., Jr. *Circular dichroism instrumentation*. In "Circular dichroism and the conformational analysis of biomolecules" (G.D. Fasman, ed.). Plenum Press, New York

56. Hicks, R. P.; Russell, A. L. *Methods Mol Biol*. **2012**, 794, 135-67.